Modeling Bose-Einstein correlations via elementary emitting cells

Oleg Utyuzh[*] and Grzegorz Wilk[†]

The Andrzej Sołtan Institute for Nuclear Studies, Hoża 69, 00-681 Warsaw, Poland

Zbigniew Włodarczyk[‡]

Institute of Physics, Świętokrzyska Academy, Świętokrzyska 15, 25-405 Kielce, Poland
(Received 9 February 2007; published 30 April 2007)

We propose a method of numerical modeling Bose-Einstein correlations by using the notion of the elementary emitting cell (EEC). They are intermediary objects containing identical bosons and are supposed to be produced independently during the hadronization process. Only bosons in the EEC, which represents a single quantum state here, are subjected to the effects of Bose-Einstein (BE) statistics, which forces them to follow a geometrical distribution. There are no such effects between particles from different EECs. We illustrate our proposition by calculating a representative number of typical distributions and discussing their sensitivity to EECs and their characteristics.

I. INTRODUCTION

In every high energy collision experiment, a vast number of secondaries (mostly pions) is produced encoding valuable information on the dynamics of the hadronization process. Because of their complexity, such reactions can only be investigated by numerical modeling using specialized codes, Monte Carlo event generators (MCEG) [1]. They all use positively defined probabilities to describe the particle production process. This means that they neglect off-diagonal terms in the corresponding density matrices formally describing such processes. As a result, they did not properly implement all the correlations, in particular, the quantum mechanical correlations between identical particles [both of Bose-Einstein type for identical bosons (BE) and of Fermi-Dirac type for identical fermions (FD)]. The whole collision process is expressed only by the product of single particle distributions. This makes the present MCEG *a priori* impossible to properly account for results of many experiments (starting from [2]), which explicitly show features usually attributed to correlations of this type [3]. To describe such experiments, one has to introduce, in some way, effects of quantum statistics, opening thus a new subject—*Bose-Einstein* (BEC) or *Fermi-Dirac* correlations [3].

This subject already has a long and well documented history [3] but it is still far from complete. Its most specific features one is faced with are the following: In experiments of an exclusive type (measuring all produced secondaries, as in [2]), it is possible (at least in principle) to construct the properly symmetrized wave function of *all* identical pions and thus account for our inability to determine which particle is emitted from which position in the source. In the simplest approach using a plane waves representation of

particles, such a wave function for the n_π-pion state has the form [4]

$$\Psi_{\{p\}}(\{x\};\{r\}) = \frac{1}{\sqrt{n_\pi!}} \cdot \sum_\sigma \exp\left[-i\sum_{j=1}^{n_\pi} p_j r_{\sigma(j)}\right] \quad (1)$$

[$\sigma(j)$ denotes the jth element of permutation of the sequence $\{1, 2, \ldots, n_\pi\}$ and we sum over all $n_\pi!$ permutations in this sequence, including the identity permutation]. Points of detection, x's, will vanish when calculating probabilities, but points of production of secondaries, r's, will remain. Because experiments measure only momenta of particles, one must integrate over $\{r_j\}$ using some multiparticle spatiotemporal distribution function, $\rho(\{r_j\})$. This is usually *assumed* to be factorizable, i.e., expressed by the product of independent single particle distributions, $\rho(\{r_j\}) = \prod_j \rho(r_j)$ [4]. Assuming further a totally chaotic hadronizing source, one gets the probability of the n_π-pion state in the form of a *permanent* of the matrix $\|\Phi_{ij}\|$,

$$\mathcal{P}_{1,..,n_\pi} = \frac{1}{n_\pi!}\sum_\sigma \prod_j \Phi_{j,\sigma(j)} = \text{perm}\|\Phi_{ij}\| =$$

$$\equiv \frac{1}{n_\pi!}\left\| \begin{matrix} \Phi_{1,1} & \cdots & \Phi_{1,n_\pi} \\ \vdots & \Phi_{j,j} & \vdots \\ \Phi_{n_\pi,1} & \cdots & \Phi_{n_\pi,n_\pi} \end{matrix} \right\|, \quad (2)$$

with

$$\Phi_{ij} = \int e^{iq_{ij}r}\rho(r)d^4\{r\}, \qquad q_{ij} = p_i - p_j \quad (3)$$

[which are all real if $\rho(r) = \rho(-r)$].

However, most modern experiments are of an *inclusive* type as one measures the effect of BEC on limited samples of secondaries only. The unobserved part of the system acts then as a kind of *thermal bath* influencing measured samples of data [5]. Also the registered multiplicities are much higher prohibiting calculation of permanents given

[*]Electronic address: utyuzh@fuw.edu.pl
[†]Electronic address: wilk@fuw.edu.pl
[‡]Electronic address: wlod@pu.kielce.pl

by Eq. (1). The subsystem subjected to further experimental (and theoretical) analysis forms only a (not too well defined) part of the total system with strongly fluctuating characteristics to be averaged during the data collection procedure. Because, as we have mentioned, such systems can be described only by numerical modeling, one faces the fundamental question of how to account for BEC in such modeling processes? It must be realized that this is a completely different thing than a simple calculation of the usually considered $n_\pi = 2$ case, which in the case considered here amounts to a well-known expression for the 2-particle BE correlation function defined as a ratio of a two particle distribution and single particle distributions with $Q = |p_i - p_j|$,

$$C_2(Q) = \frac{N_2(p_i, p_j)}{N_1(p_i)N_1(p_j)} = 1 + \left| \int dr \rho(r) \cdot e^{iQr} \right|^2$$
$$= 1 + |\tilde{\rho}(q = Q \cdot R)|^2 \qquad (4)$$

($C_2 \to 2$ when $Q \to 0$ and $C_2 \to 1$ for large values of Q) [3,6–8]. In fact, in the majority of the cases, one is following precisely this route with different functional forms of $\tilde{\rho}(QR)$ and sometimes even with an entirely different form of C_2 (cf., for example, [9]), but always derived in some analytical way—both for one- and three-dimensional cases. One is then fitting such correlation functions to appropriate sets of data, aiming to get information on the quantity R (and similar others). The reason for this is that $C_2(Q)$ is usually regarded as a (kind of) Fourier transform of the space-time characteristic of the emitting source, $\tilde{\rho}$, therefore providing information on $\rho(r)$ [10].

It is precisely this fact that makes BEC so interesting, but we shall not follow this route here. Our aim is to provide an algorithm that could cope with BEC from its first steps (to *model* it) and which could bring this effect to other MCEGs once implemented there. This we shall do by using the notion of the elementary emitting cell (EEC) introduced some time ago [11]. They are some intermediary objects (in fact quantum states) containing identical bosons (henceforth we shall assume them being pions), which are supposed to be produced independently during the hadronization process. Only bosons in EECs are subjected to Bose-Einstein (BE) statistics, which makes them follow a geometrical distribution. There are no such effects between particles from different EECs. Using this idea, we propose an algorithm that can be used in any MCEG, which has effects of BEC as one of its basic features. This will be presented on the background of previous attempts to model BEC discussed in [4,12–15]. We shall illustrate its action by calculating a representative number of typical distributions and discuss their sensitivity to EECs and their characteristics. In this work no comparison with experimental data is offered, we limit ourselves only to a thorough discussion of our algorithm. It is supposed to be the main building block of any serious MCEG aiming for a real comparison with data and including therefore, for

example, also the distribution of energies one is supposed to hadronize or possible flows in the system, i.e., subjects which are out of the scope of this work. In particular, it will be most useful in cases where the hadronizing source is well defined (as in e^+e^- annihilation processes and other elementary processes) or where the number of secondaries is exceptionally large (in high multiplicity events).

For completeness, in Sec. II we shall provide a short overview of numerical modelling of BEC proposed so far. This will put our investigation in proper perspective. Section III contains details of the proposed algorithm and examples of results obtained from its simplest version. The last section contains conclusions and a discussion. Some specific problems connected with the method proposed are addressed in Appendices A, B, and C.

II. HISTORY OF NUMERICAL MODELING OF BEC

A. Imitating BEC with existing MCEGs

Imitating BEC means to use the original outputs of the existing MCEG codes and change them in such way as to reproduce measured $C_2(Q)$ (or other experimental characteristics of BEC). Two approaches are used for this. In the first one, one introduces some special global weights (i.e., weights built for the whole event) to bias accordingly the original results of MCEG [16] (usually checking whether other observables were not changed too much—otherwise one has to rerun MCEG with new input parameters). This procedure is justified by noticing the following [17]: Let $M = \sum_\sigma M_\sigma$ be the matrix element describing the production of a hadronic final state of n identical bosons. It consists of $n!$ terms, each corresponding to a particular permutation σ of the n identical particles in the final state. In the simulation process of MCEG the interference terms [off-diagonal elements in permanent Eq. (2)] are neglected and one gets that the probability to produce such a state is

$$|M|^2_{\text{MCEG}} = \sum_\sigma |M_\sigma|^2 \leq |M|^2. \qquad (5)$$

To remedy this situation, one *assumes* some weight $\mathcal{W}_\sigma$ assigned to each event such that

$$|M'|^2_{\text{MCEG}} = \sum_\sigma \mathcal{W}_\sigma |M_\sigma|^2. \qquad (6)$$

There is no unique way to choose the weights $\mathcal{W}_\sigma$. The only requirement is that one gets good fits to the corresponding C_2 functions [16,17]. The tacit understanding is that then also $|M'|^2_{\text{MCEG}} \simeq |M|^2$.

In the second approach, one locally modifies (by weighting each pair of particles in a given event) the original output of the MCEG used. This can be done either by modifying its energy-momentum spectra [18] or by changing the resulting charge assignment [19,20]. In the first case, one introduces weight function $f_{\text{BE}}(q)$ for a pair of particles momenta which are changed, such that

$$\int_0^Q d\Omega(q) = \int_0^{Q+\delta Q} f_{\mathrm{BE}}(q)d\Omega(q), \qquad (7)$$

i.e., for $f_{\mathrm{BE}}(q) > 0$ one has $\delta Q < 0$. In this way the energy-momentum imbalance that results from such a procedure is properly accounted for and the number of particles, $N = \int d\Omega$, is conserved [18]. In the second case [19,20] the original spatiotemporal and energy-momentum structure of the original event is preserved, but often spurious unlike particle correlations occur [21]. What must be stressed is that this approach, contrary to the previous one, always works on the level of a single event. It is therefore more suitable as an additional tool (sometimes called *afterburner*) to be used together with the known MCEGs.

It must be stressed that all these methods modify original physics underlying MCEGs in an essentially unknown way [22]. Using them one *assumes* therefore that changes incurred are small and irrelevant. We shall proceed now to attempts to *simulate* BEC by which we understand a situation in which the algorithm introducing effects of quantum statistics involves *all produced particles* [4,12,14,15].

B. Attempts to simulate BEC numerically

1. Metropolis importance sampling method

In [4], the standard Monte Carlo technique due to Metropolis (*Metropolis importance sampling method*) was used. This is a general method to generate an ensemble of n-body configurations according to some prescribed probability density. In [4] this technique was used to modify the directions of momentum vectors of selected particles from a system of n identical particles in order to impose the n-particle distributions derived from BE correlation functions. In particular, it was done by changing the momenta of selected particles, $p_i \rightarrow p'_i \in d^3N/dp^3$, in such a way as to maximize the probability of detection of the n_π-multiparticle state, $\mathcal{P}_{1,...,p_{n_\pi}}$, i.e. accepting a new configuration with probability $\mathbb{P} = \min\{1, P_{\mathrm{new}}/P_{\mathrm{old}}\}$, where $P_{\mathrm{old}} = \mathcal{P}\{1,...,p_i,...,p_{n_\pi}\}$ and $P_{\mathrm{new}} = \mathcal{P}\{1,...,p'_i,...,p_{n_\pi}\}$. This procedure is then repeated many times until a kind of "equilibrium" is achieved. As shown in [4], one was able in this way to generate typical multipion events, which explicitly exhibit all correlations induced by Bose statistics. The most important result for our further consideration is the fact that, as a result of the application of this algorithm a number of objects, called *speckles* in [4] and being clusters of a number of identical pions in phase-space, is formed. It means that in the multidimensional phase-space permanent (2) exhibits rich structure of local maxima (attracting particles) and voids (repulsing them), which replaces the original distribution one started from. Actually the only drawback of this method is that symmetrization of clusters with sizes larger than $n_{\mathrm{cluster}} \approx 10$ takes a prohibitively long time.

Two points must be stressed when summarizing this symmetrization procedure. The first is that it involves all (identical) secondaries in the event under consideration, some producing specific structure in their distribution in the allowed phase-space, namely, it is clustering them in some regions of phase-space. The second point is that this phenomenon leads immediately to a broadening of the resultant multiplicity distribution (MD): starting from a Poisson MD for a nonsymmetrized wave function one ends up after symmetrization with a geometrical (or Bose-Einstein) MD for a single speckle and with negative binomial MD [23] for the whole system.

We close this section with the following remark. So far, particles were represented, for simplicity, by plane waves. However, this approach leads to some unpleasant effects because it violates the Heisenberg uncertainty relation constraining the simultaneous specification of coordinates and momentum as implied by Eq. (4). For example, in the case of sources with strong position-momentum correlations the two-particle correlation function $C_2(Q)$ can drop significantly below unity [8,24]. This method has therefore been generalized in [12], where plane waves have been replaced by wave packets. Both features mentioned above were also observed here. Therefore in [13] modification simplifying the selection process was proposed. It was argued that it could be limited only to identical particles whose wave functions overlap in phase-space, i.e., to particles forming speckles or clusters mentioned above (with the size of this overlap being a new parameter). Notice that such decomposition corresponds to replacing the full permanent in Eq. (2) by matrix with a block structure, each block representing one cluster with no correlations between them:

$$\left\| \begin{array}{ccc} \mathrm{EEC}_1 & \cdots & 0 \\ \vdots & \ddots & \vdots \\ 0 & \cdots & \mathrm{EEC}_{N_{\mathrm{cell}}} \end{array} \right\|. \qquad (8)$$

In what follows we shall identify these blocks with EECs mentioned before. However, it should be remembered that cells selected here were so far preselected in (Φ, Θ) space only and, by construction, tend to contain particles with similar momenta. This method differs therefore from what we are going to describe now in which EECs are created dynamically without any restriction [14].

2. The acceptance-rejection method

The *acceptance-rejection method* used in [14] is the well-known "hit-or-miss" technique of generating a set of random numbers according to a prescribed distribution, here given by an expression describing the collapse of a multiparticle wave function into a properly symmetrized state represented by Eq. (2), as required by Bose quantum statistics. In contrast to that discussed above, this method is sequential because the n multiparticle event is constructed by adding the kth particle to the $(k-1)$ particles already

selected, until $k = n$ is reached. This is done in the following way. One starts with empty phase-space and inserts in it the first particle with momentum chosen according to some distribution (for example, the one which is supposed to reproduce single particle spectra). The presence of the first particle causes that a second particle must be added according to the 2-particle distribution function, which for identical bosons is given by the 2-particle correlation function $C_2 \propto P_{1,2}$ with momentum of the first particle fixed and momentum of the second particle to be selected. Because $C_2(Q = p_1 - p_2)$ has a maximum at $Q = 0$, the second particle will tend to be located near the first one in phase-space but *a priori* it can take any position in it. Addition of a third particle must be now performed according to $C_3 \propto P_{1,2,3}$ (with momenta p_1 and p_2 already fixed and only p_3 being selected), which again has bumpy structure, especially when particles 1 and 2 are located far from each other. Therefore the third particle will most probably locate itself near one of the already selected particles but *a priori* it can take any position in phase-space. If, by chance, it will be far away from both particles 1 and 2, it will become for future particles a new point of attraction and seed of the new bump. Notice that if, say k particles occupy the same region of phase-space, the strength of the bump they form, which attracts other particles, increases $k!$ times. This process, schematically illustrated in Fig. 1, continues until all particles are used (their number can be either preselected, in which case the initial energy will vary, or can result from the procedure itself when initial energy is fixed).

To summarize: this procedure leads again to some specific nonuniform distribution of particles in the allowed phase-space with some cell-like structures (bumps) showing up. It results from the fact that regions with some particles inside them already present will have a bigger chance to attract a new particle. Unfortunately, this sequential procedure is even more time consuming than the previous one and therefore rather unpractical.

3. Information theory approach

The only workable example of MCEG with features of Bose-Einstein statistics built in from the very beginning has been proposed in [15]. The known total energy E_{tot} has there been distributed among a given (mean) number of secondaries, $\bar{n} = \bar{n}_+ + \bar{n}_- + \bar{n}_0$ (where $\bar{n}_+ = \bar{n}_-$), with limited transverse momentum parametrized by the mean value $\langle p_T \rangle$, and it was done in such way as to reproduce data on both single particle distributions and those for BEC as well. To this end, the information theory (IT) method was used to obtain the most probable (and least biased) formula for rapidity distributions, dN/dy, and multiplicity distributions $P(n)$. It resembles the usual grand canonical distribution but is more general than that because the "temperature" T and "chemical potential" μ occurring there are now two Lagrange multipliers obtained by solv-
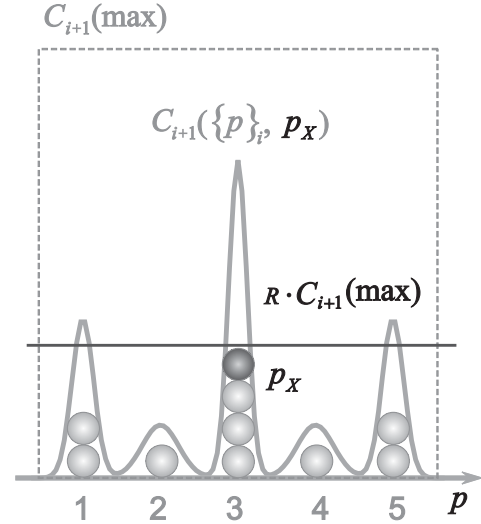

FIG. 1.   Schematic example of acceptance-rejection algorithm proposed in [14] at work; $C_{i+1}(\text{max}) = (i + 1)!$ and $R \in [0, 1]$ is a random number. For i particles already present with $p_{i=1}$ fixed (gray circles, here $i = 9$), one calculates $C_{i+1}(\{p_{1,...,i}\}, p_x = p_{i+1})$ and selects a random number R. For the situation shown here [with schematic form of $C(p_x)$ as an example], a new particle can only be added to "cells" 1, 3, and 5 but not to 2 and 4.

ing the corresponding energy and particle conservation constraints. To also get $C_2(Q)$ it turned out that it is enough to additionally divide the available rapidity space into cells of fixed size δy each and assume that each cell can contain only identical particles (i.e., pions of the same charge in this case). It is remarkable that, in addition to reproducing all single-particle characteristics of the collision as well as backward-forward correlations, with this step one gets at the same time also multiplicity distributions $P(n)$ in negative binomial (NB) form [25], the proper structure of the two-particle BEC function $C_2(Q)$ and intermittency signal [26]. The distinctive feature of this method is that it deals only with measured momenta of produced secondaries, there is no trace on the unmeasured spatiotemporal structure present in other methods. If one now wants to somehow deduce this information, one has to treat $C_2(Q)$ in the same way one is treating all experimental results on BEC [i.e., in fact one has *to assume* that it is a kind of Fourier transform of the hadronizing source $\rho(r)$ and perform its routine analysis as in [6,10,27]].

The most important result of [15] for us is demonstration that the decisive factor leading to proper structure of the correlation function $C_2(Q)$ was bunching property in the rapidity space introduced there.

C. Quantum optical analogy

Let us therefore concentrate for a moment on this bunching feature of bosons introduced in [15]. At first let us remind ourselves that it has been noticed and discussed already many times [13,28–30] and was regarded as a

manifestation of quantum statistics [31]. It is especially widely discussed and used in quantum optics [32] but it was also employed to describe some aspects of the multi-particle production processes [11,33,34]. This is because C_2 can be also regarded as some measure of correlation of fluctuations. One uses here the fact that

$$\langle n_1 n_2 \rangle = \langle n_1 \rangle \langle n_2 \rangle + \langle (n_1 - \langle n_1 \rangle)(n_2 - \langle n_2 \rangle) \rangle$$

$$= \langle n_1 \rangle \langle n_2 \rangle + \rho \sigma(n_1) \sigma(n_2) \qquad (9)$$

[where $\sigma(n)$ is dispersion of the multiplicity distribution $P(n)$ and ρ is the correlation coefficient depending on the type of particles produced: $\rho = +1$, -1, 0 for bosons, fermions, and Boltzmann statistics, respectively]. It means therefore that one can write the two-particle correlation function (4) in terms of the above covariances (9) stressing therefore its stochastic character [19,20,35]:

$$C_2(Q) = \frac{\langle n_i(p_i)[n_j(p_j) - \delta_{ij}] \rangle}{\langle n_i(p_i) \rangle \langle n_j(p_j) \rangle}$$

$$= 1 + \rho \frac{\sigma(n_i)}{\langle n_i(p_i) \rangle} \frac{\sigma(n_j)}{\langle n_j(p_j) \rangle} - \frac{\delta_{ij}}{\langle n_i(p_i) \rangle}. \qquad (10)$$

Notice that, for geometrical (Bose-Einstein) multiplicity distribution $\sigma^2(n_i) = \langle n_i(p_i)[n_i(p_i) - 1] \rangle$ (corresponding to bosons, $\rho = 1$), one gets, for $i = j$, $C_2(Q = 0) = 2$, i.e., its maximal allowed value. This bunching property has already been used in our previous proposition of MCEG of the "afterburner" type [19,20] mentioned in Sec. II A, it was realized in the form of EECs introduced in [11]. Essentially the same idea will be the cornerstone of our algorithm, which we shall now present. Identical pions will be assumed to be subjected to BEC only when inside EECs, those from different EECs are totally independent (this can be also expressed using notation *chaotic* and *coherent*, see Appendix A).

III. MODELING BOSE-EINSTEIN CORRELATIONS VIA ELEMENTARY EMITTING CELLS—OUR ALGORITHM

A. Introduction

The lesson learned from the approaches presented in Sec. II is that construction of the proper quantum multi-particle bosonic state can be performed (i) either by symmetrization of the corresponding wave function constructed for all produced particles [4,12–14] or (ii) by following quantum statistical arguments formulated in [28–30] and directly bunching produced identical secondaries with (almost) the same energy in phase-space to form EECs [11,13,15]. So far, the fact that the distribution obtained this way is of negative binomial (NBD) type was only shown in [4]. Nevertheless the emergence of bunching (both in [4,14]) is convincing and makes it an essential characteristic of the bosonic character of produced secon-

daries one has to account for. This will be our main assumption in what follows.

We have decided to *model* the effects of proper symmetrization of a multiparticle state by assuring that identical particles are produced in bunches with geometrical distribution of particles. To get such a distribution, one has to choose particles sequentially with some prescribed probability $\mathcal{P}$ until first failure. If this failure happens for the $(N + 1)$th trial, one gets immediately that

$$P(N) = (1 - \mathcal{P})\mathcal{P}^N \quad \text{with } \langle N \rangle = \frac{\mathcal{P}}{1 - \mathcal{P}}. \qquad (11)$$

Notice that for $\mathcal{P}$ defined as

$$\mathcal{P} = \mathcal{P}_0 \cdot \exp\left(-\frac{E_i}{T}\right) \qquad (12)$$

(and only then), one gets the usual form of the Bose-Einstein distribution for the ith EEC:

$$\langle N(E_i) \rangle \equiv \frac{1}{\mathcal{P}_0^{-1} e^{E_i/T} - 1}. \qquad (13)$$

Because, according to Eq. (12) $\mathcal{P}_0$ controls the maximal number of particles which can be allocated in a given EEC, one can formally introduce a kind of "chemical potential" (as in [15]) defined as $\mu = T \ln \mathcal{P}_0$ and get [36]

$$\langle N(E_i) \rangle = \frac{1}{e^{(E_i - \mu)/T} - 1}. \qquad (14)$$

Such a choice of $\mathcal{P}$ is therefore very crucial in the process of further modeling BEC and is thus the cornerstone of our algorithm.

Let us now demonstrate this procedure on a simple example of a one-dimensional pionic lattice model [20]. The pions located in the sites of the lattice (which prevents identical pions to be found at the same point of phase-space) are endowed with charges in such way that, after selecting the charge of the first pion, one assigns the same charge to the consecutive neighboring pions with probability $\mathcal{P}$ until first failure. After failure, one assigns (again randomly chosen) charge to the next pion in line and continues this procedure until all pions are used. In this way a number of cells is formed with particles in them distributed *by construction* [cf. Eq. (11) and [36]] in geometrical fashion, cf., Fig. 2. In Fig. 2(a) dependence of C_2 on the lattice spacing defined by different values of N is presented whereas Fig. 2(b) presents its dependence on Q defined as

$$Q = | p_i - p_j | = \frac{2p_{max}}{N} \cdot | i - j | = \delta p \cdot n \qquad (15)$$

(where $p \in [-p_{max}, p_{max}]$ with $p_{max} = 10$ GeV and $N = 100$ denotes the total number of sites in our lattice). Comparing them, one can deduce that the width of the correlation function, $\sigma(C_2)$, is roughly proportional to the product of the average number of particles in the cell,
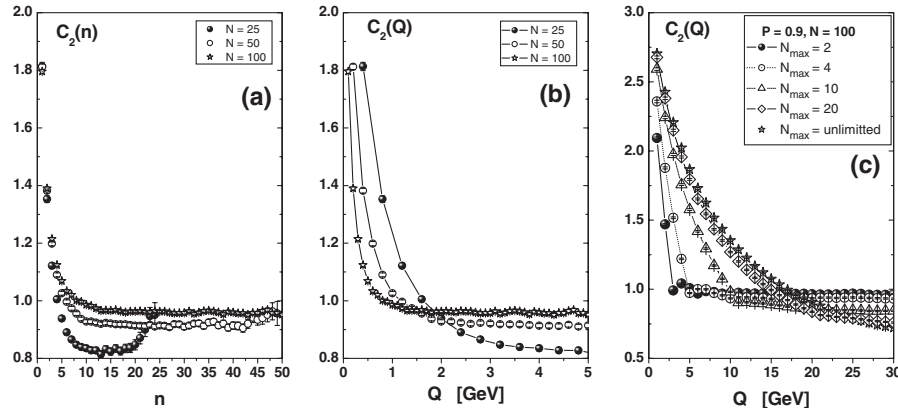
FIG. 2. Example of C_2 occurring for a pionic lattice in (one-dimensional) momentum space: (a) $C_2(n)$ as function of the number of particles in a given cell for different N; (b) $C_2(Q)$ as function of Q (in both cases $\mathcal{P} = 0.5$). In (c) $C_2(Q)$ as a function of Q defined by Eq. (15) for artificially limited cell occupancy, $i < n_{\max}$ (now $\mathcal{P} = 0.9$).

$\langle N_{\text{part}} \rangle$, and the average distance $\langle \delta p \rangle$ between these particle on the lattice, $\sigma(C_2) \propto \langle N_{\text{part}} \rangle \cdot \langle \delta p \rangle$. Because the average distance between particles on the lattice is fixed by the (constant) lattice spacing, the width of the correlation function depends only on the mean cell occupancy, $\langle N_{\text{part}} \rangle$, which is directly related to the probability $\mathcal{P}$ [cf. Eq. (13)] and for constant $\mathcal{P}$ all widths of $C_2(n)$ in Fig. 2(a) are the same. Finally, in Fig. 2(c) the correlation function $C_2(Q)$ is shown for different limits $N_{\max}$ imposed on the maximal allowed cell occupancy ($i < N_{\max}$) (for $\mathcal{P} = 0.9$ to assure large occupancy of EECs). Notice that both the value of the intercept parameter, $\lambda = C_2(Q = 0) - 1$, and the width of the correlation function C_2 depend on the maximally allowed number of pions in one cell, $N_{\max}$.

B. Implementation

This experience prompted us to propose that BEC should be introduced into the modeling procedure of multiparticle production processes as early as possible, ideally at the very first stage of the selection procedure. It means that one must devise some procedure how to divide a given amount of energy W into produced bosonic particles, assumed to be pions of charges: $(+, -, 0)$, without any *a priori* assumption on what concerns their multiplicities other than $n^{(+)} = n^{(-)}$ but with effects of quantum statistics accounted for. Among procedures mentioned above only that in Sec. II B 2 [14] satisfies this demand; however, because it always involves all produced particles, it very quickly becomes impossible to follow because of CPU time demand. On the other hand, results of [4,14] show explicitly that quantum statistics leads to bunching particles in phase-space. Such bunching was therefore assumed in [12,13,15] and in [15], for the first time, the geometrical distribution form of particles in bunches was used [25].

We shall assume therefore that particles are produced according to a mechanism which can be regarded as a quantum version of the *clan model* (CM) introduced in

[23] to explain the fact that apparently all multiparticle production processes result in the NB form of resulting multiplicity distributions $P(N)$; we call it therefore the *quantum clan model* (QCM), cf. Fig. 3. In the CM model (distinguishable), particles are supposed to be produced in clans, which were supposed to be formed independently (and therefore distributed in Poisson fashion), with particles in clans following a logarithmic distribution. Convolution of these two results in the NB form of $P(N)$ ($\mathcal{P}$ denotes the probability of producing a particle),

$$P_{\text{NB}}(N) = \binom{N + k - 1}{k - 1} \mathcal{P}^k (1 - \mathcal{P})^N. \tag{16}$$

In QCM, because of quantum statistics, we must assume that each quantum clan represents a single quantum state and therefore contains only identical particles of (almost) the same energy, which are distributed geometrically [11,15,28]. Keeping the assumption of independent production of quantum clans, one immediately finds that previous NB multiplicity distribution (16) is now replaced by the so-called Pólya-Aeppli (geometric-Poisson) distribution defined as [37] [with $\Theta = (1 - \mathcal{P})\langle N \rangle$]
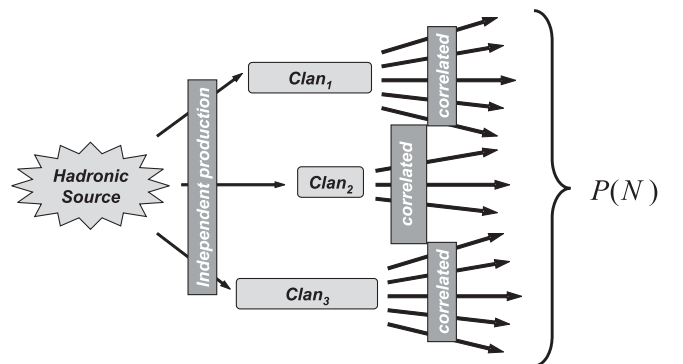

FIG. 3. Schematic view of *quantum clan model* (QCM).

$$P_{\mathrm{PA}}(N) \equiv \mathrm{Poisson} \bigotimes \mathrm{geometrical}$$

$$= e^{-\Theta} \mathcal{P}^N \sum_{j=1}^{N} \binom{N-1}{j-1} \frac{[\Theta(1-\mathcal{P})/\mathcal{P}]^j}{j!}, \quad (17)$$

which was already used in multiparticle phenomenology some time ago [38]. It differs from the NB only at small multiplicities. Otherwise it is essentially the same.

To numerically implement the QCM we proceed in the following way.

(i) A pion of randomly chosen charge is selected with energy $E_1 = E_{\mathrm{EEC}}$ following some assumed distribution $f(E)$. The form of this distribution is dictated by physics of the model used to describe the production process which we would like to follow (much the same as in [14]). It has no influence on the bosonization (other then emerging from conservation laws); on the other hand, it strongly affects the final form of multiparticle distributions obtained (by changing effective distributions of EECs). This pion is therefore supposed to be the *seed* for the first EEC.

(ii) The other pions of the same charge are then added, one after another, using probability $\mathcal{P}$ as given by Eq. (12). This is done until the first failure, which marks the end of formation of the first EEC. After that, one starts formation of another EEC by proceeding to point (i) and choosing from $f(E)$ another energy E_{EEC} of another pion of randomly chosen charge, which forms the seed of the second EEC. The whole procedure is repeated until all available energy M is used up.

(iii) Once accepted, each of the selected pions forming the first EEC is endowed with energy E_i ($i \geq 2$),

which is selected from some distribution $G(E_i)$ centered on the energy of the first pion forming the seed of this EEC, E_{EEC}. The sense of the function $G(E_i)$ is that it reflects the fact that the requirement that all particles belonging to a given EEC must be in the same energy state, in which case one expects that $G(E_i) \sim \delta(E_{\mathrm{EEC}} - E_i)$ means that their energies can differ only by an amount corresponding to the width of the spectral line mentioned in [29]. We shall then use $G(E)$ either in the form of delta function mentioned above or parametrize it by a Gaussian,

$$G(E_i) = \frac{1}{\sqrt{2\pi}\sigma} \exp\left[-\frac{(E_{\mathrm{EEC}} - E_i)^2}{2\sigma^2} \right]. \quad (18)$$

In the thermal-like model for $f(E)$ used here, there is a natural length scale given by the temperature T and it is therefore natural to choose σ as being proportional to it, we shall therefore take $\sigma = \sigma_0 T$ (for the possible physical meaning of σ see Appendix B).

In this work we shall use the function $f(E)$ in the form of a Boltzmann distribution,

$$f(E) = \exp\left(-\frac{E}{T}\right), \quad (19)$$

corresponding to a kind of thermal-like model with temperature T being the main parameter. In this case the parameter $\mathcal{P}_0$, governing the number of particles in EECs, plays the role of the chemical potential. As expected, one gets then EECs distributed according to a Poisson distribution, each EEC containing particles of the same charge only, which are distributed according to Bose-Einstein (or geometrical) distribution, also the shape of charged particle multiplicity distributions comes out as expected, see Fig. 4. It was obtained for hadronizing energy
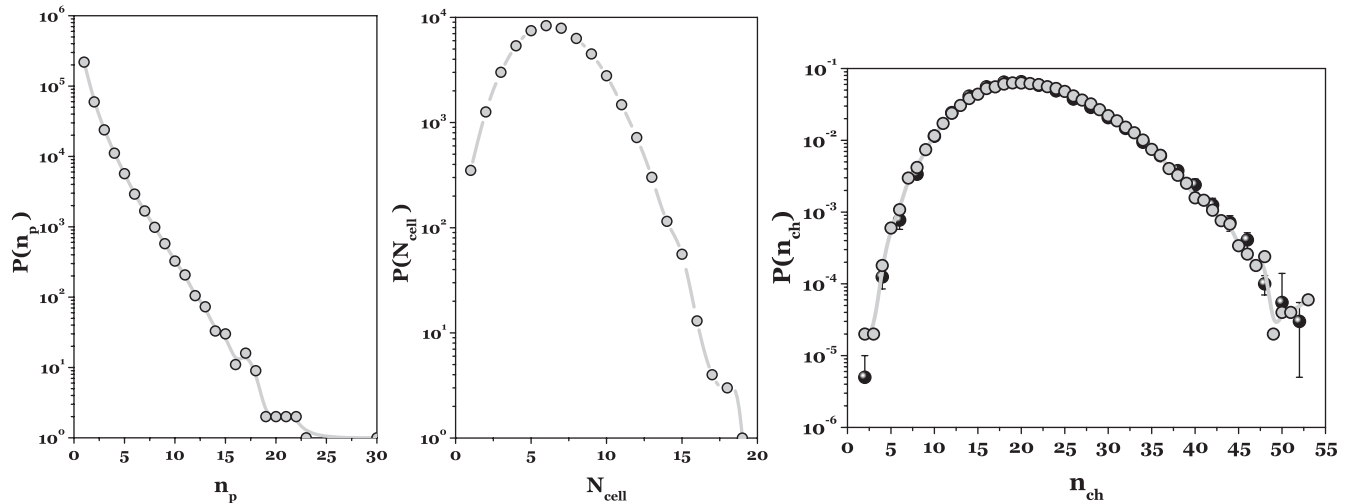

FIG. 4. Examples of the distribution of particles in a given EEC (left panel), distribution of EECs (middle panel), and total charged particle distribution resulted from the convolution of distributions shown in the first two panels (right panel, open circles and solid curve, see text for details). Notice that, with this choice of parameters, one can reproduce exactly the experimental data for $e^- e^+$ annihilations taken at the same energy [57] (black circles).

TABLE I. The mean total multiplicities and their dispersions ($\langle N \rangle$ and σ_N), the mean total multiplicities of EECs and their dispersions ($\langle N_{\text{cell}} \rangle$ and $\sigma_{N_{\text{cell}}}$), and mean multiplicities and dispersions in EECs ($\langle N_{\text{part}} \rangle$ and $\sigma_{N_{\text{part}}}$) calculated for some selected choices of parameters $\mathcal{P}_0$ and T (upper part) and for different initial energies [$W(\text{i}) = 0.5W$, $W(\text{ii}) = W = 91.2$ GeV, and $W(\text{iii}) = 2W$—lower part]. All results are for $\sigma_0 = 0.0$ except the middle part, which was obtained for $\sigma_0 = 0.3$ for comparison.

$\mathcal{P}_0$	T	$\langle N \rangle$	σ_N	$\langle N_{\text{cell}} \rangle$	$\sigma_{N_{\text{cell}}}$	$\langle N_{\text{part}} \rangle$	$\sigma_{N_{\text{part}}}$
0.9		41.39	12.87	18.21	3.24	2.27	2.61
0.7	3.5	33.81	8.28	20.58	3.73	1.64	1.28
0.5		30.34	6.63	22.41	4.11	1.35	0.78
0.3		28.22	5.69	24.01	4.44	1.17	0.48
	1.5	82.68	15.29	39.85	4.66	2.07	2.13
0.9	3.5	41.39	12.87	18.21	3.24	2.27	2.61
	5.5	27.99	11.13	12.03	2.64	2.32	2.78
0.7	3.5	32.05	7.12	19.54	3.47	1.63	1.27

W	$T \; \mathcal{P}_0$	$\langle N \rangle$	σ_N	$\langle N_{\text{cell}} \rangle$	$\sigma_{N_{\text{cell}}}$	$\langle N_{\text{part}} \rangle$	$\sigma_{N_{\text{part}}}$
(i)	3.5	21.22	9.08	9.49	2.29	2.24	2.56
(ii)	0.9	41.39	12.87	18.21	3.24	2.27	2.61
(iii)		81.70	18.27	35.62	4.58	2.29	2.65

$W = 91.2$ GeV using $T = 3.5$ GeV, $\mathcal{P}_0 = 0.7$, and $\sigma_0 = 0.3$. For the corresponding values of mean multiplicities and their dispersion cf. Table I (the middle row).

The $W = 91.2$ GeV value of energy will be used throughout the paper (chosen to allow for the only comparison with data we show in Fig. 4). In all examples shown here the number of MC trials was $N_{\text{MC}} = 50\,000$ and a

reference frame used to calculate the C_2 function is composed from $(+-)$ particles whereas C_2 themselves are calculated for $(--)$ pairs. Table I shows the corresponding multiplicities (and their dispersions) of all particles obtained when hadronizing mass W and those for the total number of EECs and particles in them. The bigger $\mathcal{P}_0$, the bigger the total multiplicity, smaller the number of EECs, and bigger their occupancy. Increase of T decreases the total multiplicity and the number of EECs but slightly increases their occupancy. The increase of available energy W results in an increase of all these quantities, except for the cell occupancy, which remains essentially the same.

Figure 5 shows an example of the corresponding energy distributions of produced secondaries. Notice that the effect of bunching (i.e., effect of introducing EECs) is visible only in the limited range of the allowed phase-space, concentrated at small energies. In the case considered here, where the allowed range is $(1/2) \cdot (W = 91.2)$ GeV, it practically vanishes for $E > 7.0$ GeV and after that value the distribution follows the exponential form of $f(E)$ we have started from. This means that BEC increases the multiplicity of the event by adding particles with small energies (see also Table II). Notice that for nonzero σ_0 one gets a displaced maximum for small values of E. At large energies results follow the shape of the original $f(E)$ distribution (19) used here. The other important feature is the fact that none of the numerical simulations reproduces the Bose-Einstein form of energy dependence of occupation number, usually used in all analytical estimations and given by Eq. (13). This is because of the finiteness of available energy W one can use for hadronization, which results in limited occupancy of
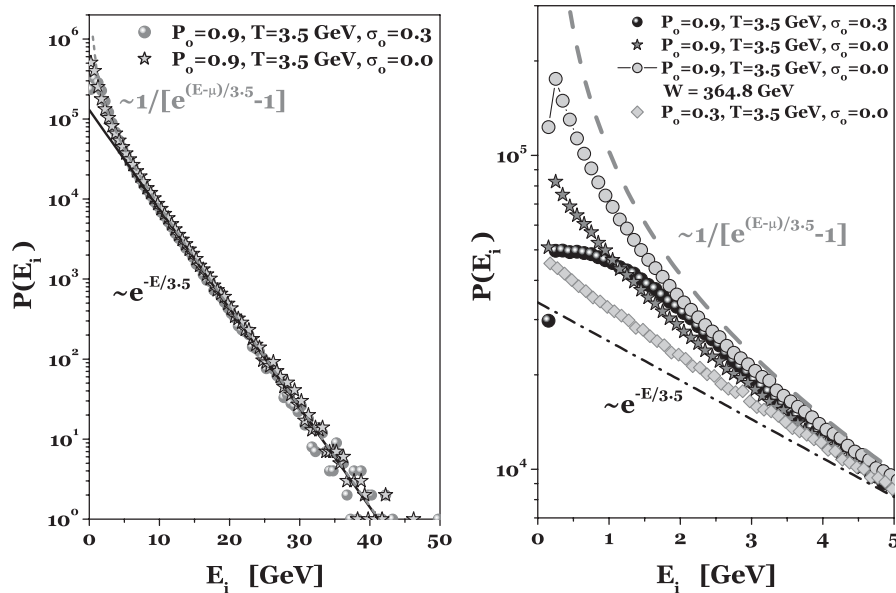

FIG. 5. Comparison of energy distributions obtained using zero and nonzero values of σ_0 compared (dashed line) with the corresponding Bose-Einstein form of energy dependence of occupation number as given by Eq. (13). The mass of hadronizing source is $W = 91.2$ GeV, except the last curve where it is 4-fold greater for comparison.

TABLE II.   The mean number of EECs, N_{cell}, and charged particles multiplicity in them, n_{π^-}, in different energy bins calculated for $T = 3.5$ GeV and two sets of (σ_0, $\mathcal{P}_0$).

Bins in E (GeV)	$\sigma_0 = 0.1$; $\mathcal{P}_0 = 0.9$		$\sigma_0 = 0.3$; $\mathcal{P}_0 = 0.7$	
	N_{cell}	n_{π^-}	N_{cell}	n_{π^-}
0.0–0.5	0.58	2.62	0.63	1.2
0.5–1.0	0.72	3.00	0.79	1.60
1.0–2.0	1.16	2.98	1.26	2.62
2.0–3.0	0.87	1.58	0.95	1.70
3.0–5.0	1.15	1.64	1.25	1.76
5.0–7.0	0.65	0.77	0.71	0.83
>7.0	0.84	0.89	0.92	0.97

EECs and violates conditions used to obtain Eq. (13) [36]. Detailed results on the mean number of EECs and charged particles multiplicity in them in different energy bins are presented in Table II.

We now proceed to the correlation functions $C_2(\delta_X = X_1 - X_2)$ and start with distributions in energy, $C_2(\delta_E)$. In Fig. 6, one observes that, when using $\sigma_0 = 0$ [i.e., for the strictly δ-like form of $G(E)$], the whole effect is located in the first bin only (this is just computer realization of delta function). Therefore, if nonzero widths of C_2 are needed, one must use $\sigma_0 > 0$. Notice, however, that this width is not equal to the input $\sigma = \sigma_0 T$ used because the difference of two variables, each following the same Gaussian distribution, is again Gaussian but with twice σ^2, therefore the final distribution should be $\sim\sqrt{2}$ broader, which is roughly the case shown in Fig. 6 [where $\sigma = 0.35$ GeV was used as input in (18) whereas the width which can be read off from the obtained shape of C_2 is equal to 0.45 GeV].
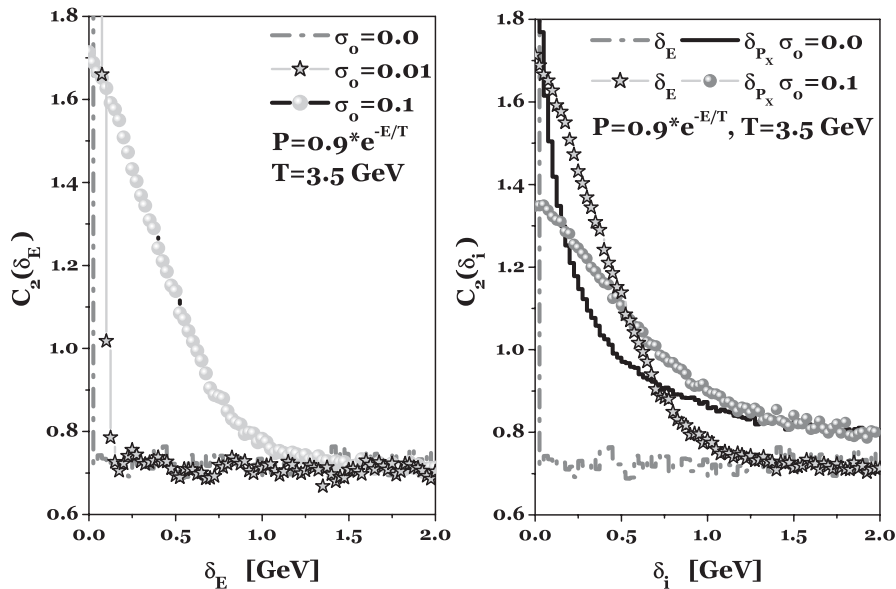
We must stop for a moment to comment on the fact that, in all figures presenting $C_2(\delta_X)$ shown here, their values are significantly smaller than unity for large values of δ_X. This is not an artifact of our algorithm, but results from the method of presentation of our output. We want to keep the same number of pairs both in the real event and in the reference one (which, in our work, is always built from pairs of opposite charges). Technically it means that one has to conserve the area under each curve for $C_2(\delta_X)$. Actually this effect is also known in all other approaches to BEC and is usually corrected by arbitrarily shifting C_2 in such a way that it equals unity for some large value of the argument (in practice set to be equal to 1 GeV) [16]. We shall not do this here, but this fact must be remembered when looking at our results.

In Fig. 6 $C_2(\delta_E)$ is compared with $C_2(\delta_{p_x})$ calculated assuming an isotropic distribution of momenta of particles in a given EEC, $\vec{p}$. The freedom presented in the choice of directions of momenta results in a nonzero width of the otherwise δ-like structure of $C_2(\delta_E)$ for $\sigma_0 = 0$. It then further broadens when one allows for some nonzero width σ_0. This means that it can be used as an additional parameter when comparison with data would be attempted (provided its physical meaning will be made clear, see, for example, the discussion in Appendix B and [39]).

If one wants to further continue with $C_2(\delta_{p_{x,y,z}})$, some additional input [new parameter(s)] is necessary, which has to be justified. We shall not discuss this point in detail, as it would bring us outside the main scope of this paper. Instead, we limit ourselves to showing in Fig. 7 the results of some more refined choices of directions of momenta.
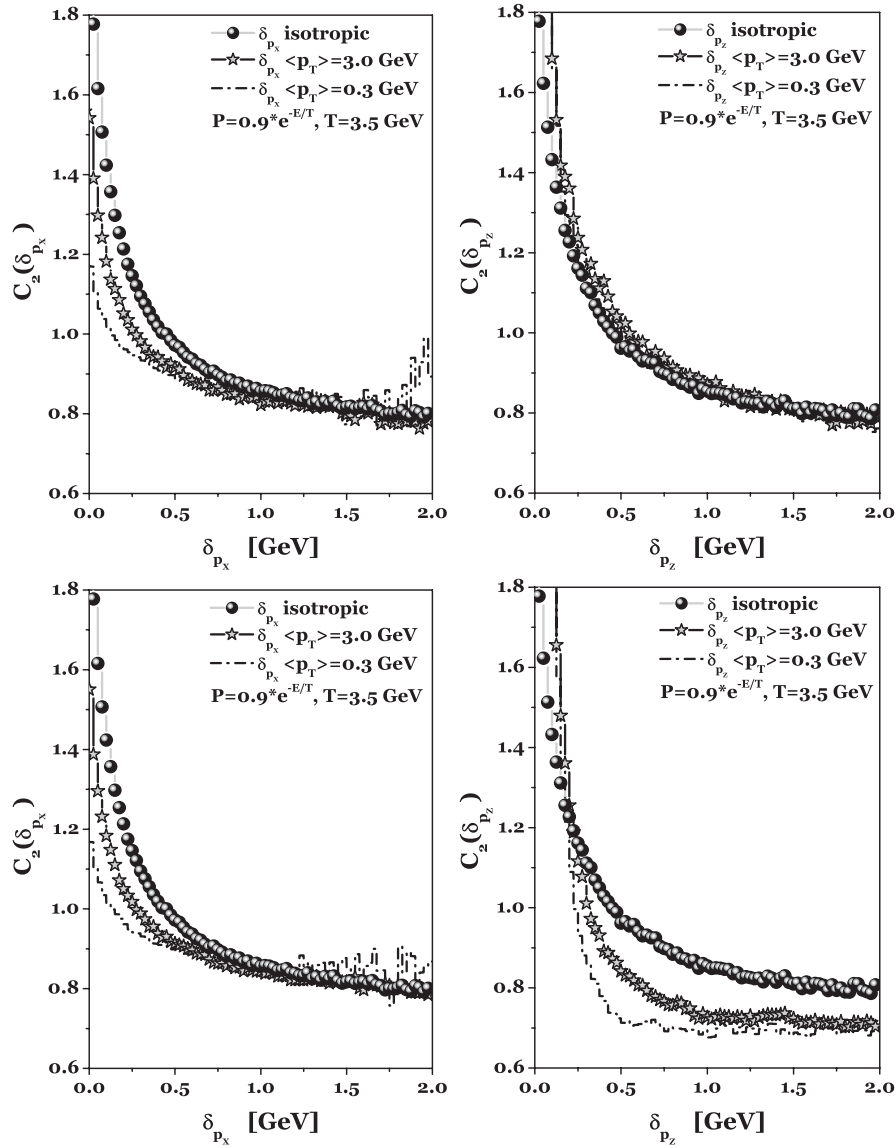

FIG. 6.   Illustration of importance of spreading in energy. Left panel: $C_2(\delta_E)$ case with $\sigma_0 = 0.0$, 0.01, and 0.1. For $\sigma_0 = 0$ the maximum of C_2 is divergent (all points are in the first bin). Right panel: $C_2(\delta_{E,p_x})$ cases with $\sigma_0 = 0.0$ or $\sigma_0 = 0.1$. Notice that $C_2(\delta_{p_x})$ (calculated for momenta distributed isotropically) has nonzero width even for $\sigma_0 = 0$. Introducing nonzero σ_0 results in further broadening of C_2.

FIG. 7. Comparison of two different ways of choosing momenta of particles occupying given EECs ($|\vec{p}|$ is always fixed) for δ_{p_x} (left panels) and δ_{p_z} (right panels). Upper panels: the $(+, -)$ sign of p_L was chosen randomly for every particle without referring to the EEC it belongs to. Lower panels: it was chosen randomly for EECs and kept the same for all particles in it. In all cases three choices of p_T is shown: unlimited (*isotropic*) and with limits imposed by two different values of $\langle p_T \rangle$ when sampling p_T from exponential distribution; in all cases $\sigma_0 = 0$.

All results are for $\sigma_0 = 0$, introduction of nonzero σ_0 will change them accordingly in the manner presented in Fig. 6. They were obtained by choosing first values of transverse momenta, $p_T = |\vec{p}_T|$, by selecting them from some exponential distribution constrained only by the assumed mean value, $\langle p_T \rangle$, which serves therefore as a new parameter. This corresponds to selection of polar angles from the band centered on $\Theta_{\text{mean}} = \arctan(\langle p_T \rangle / p_L^{(\text{max})})$, the corresponding axial angles were chosen uniformly from the $[0, 2\pi]$ range. In this way, one gets components p_x and p_y and longitudinal component $p_z = p_L = \pm\sqrt{p^2 - p_T^2}$. Two natural situations are considered here: (i) the maximally

isotropic case [the p_L of every consecutive particle, irrespective of the EEC they belong to, is randomly assigned the sign $(\pm)$] and (ii) the case in which bunching in energies is preserved also on the level of momenta (all particles in a given EEC have p_L in the same hemisphere). All other choices should interpolate between these two.

Two characteristic features seen in Fig. 7 should be noticed: (i) one observes narrowing of $C_2(\delta_{p_x})$ (i.e., transverse) distributions with tightening the allowed p_T region (i.e., when proceeding from fully isotropic distributions to those restricted by assumed $\langle p_T \rangle$ with diminishing values of $\langle p_T \rangle$), this effect is essentially independent of the way the signs of p_z components are chosen. (ii) $C_2(\delta_{p_z})$ shows

different behavior depending on which choice of signs is followed: it shows no dependence on $\langle p_T \rangle$ for the choice (i) above whereas for the choice (ii) a difference shows up only for $\delta_{p_z} > 0.2$ GeV. The situation changes dramatically when one allows for smearing of energy in the EEC, i.e., for $\sigma_0 > 0$, see Fig. 8. This means introducing a new parameter, to which our results are most sensitive but which is still not well understood (see, for example, Appendix B).

In Fig. 9 results for $C_2(\delta_E)$ and $C_2(\delta_{p_x})$ are compared with those for $C_2(Q_{\mathrm{inv}})$, where $Q_{\mathrm{inv}}^2 = -(p_1 - p_2)^2$ with $p_{1,2}$ being 4-momenta of particles 1 and 2 (it is relativistically invariant variable , such that $Q_{\mathrm{inv}}^2 = 0$ implies for massive particles that $\vec{p}_1 = \vec{p}_2$ and BEC has its maximum there). Notice the peaked shape of $C_2(Q_{\mathrm{inv}})$ and the fact that $C_2(Q_{\mathrm{inv}} = 0) > 2$ here. As shown in [40] both features

are mostly due to the specific kinematics of the Q_{inv} variable (because of which it collects in the first bin contributions from the whole range of momenta provided only that they are near enough to each other). The point is that in the case of Q_{inv} variable smearing σ in energy E and smearing in momentum p are not independent and therefore they do not sum up (as is the case for independent variables) but rather they tend to cancel. In fact, their global effect is of the order of $\sigma \cdot (\sqrt{p^2 + m^2} - p)$ which tends to zero for large momenta and never exceeds $\sigma \cdot m$, where m is pion mass. In other words, smearing in Q_{inv} is considerably smaller than that in energy and momentum. Therefore there is a natural tendency of increasing occupancy of the lowest bins in $\delta_i = Q_{\mathrm{inv}}$ in comparison to δ_E or δ_{p_x}.
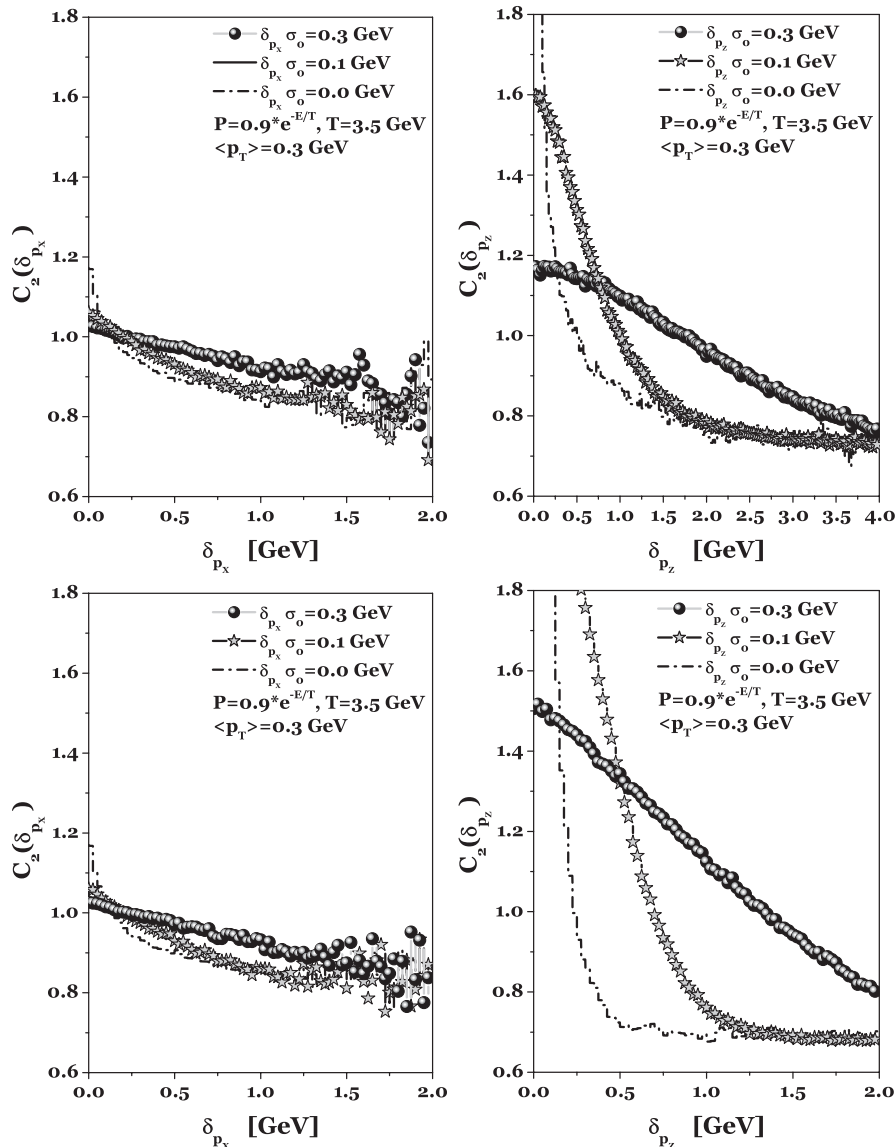

FIG. 8. The same as in Fig. 7 but for choice of p_T restricted by $\langle p_T \rangle = 0.3$ GeV and for different values of $\sigma_0 = 0.0, 0.1,$ and 0.3.
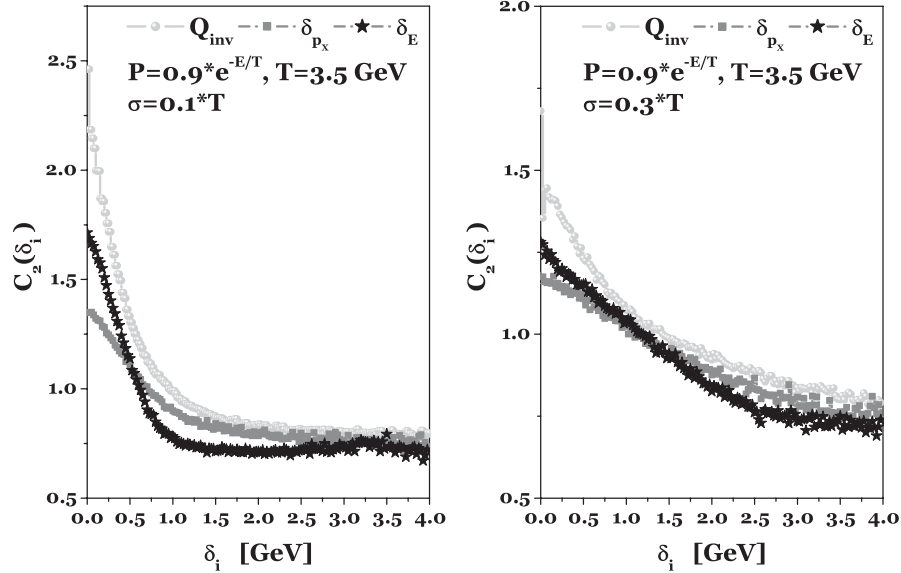
FIG. 9.   Comparison of $C_2(\delta_i = \delta_{E,p_x})$ as presented in Fig. 6 for $\sigma_0 = 0.1$ with $C_2(\delta_i = Q_{inv})$ for the same parameters (left panel). Notice that the maximum of $C_2(Q_{inv} = 0) > 2$, and to get it below this value one has to increase σ_0 (see right panel with $\sigma_0 = 0.3$).

Let us now stress the most specific feature of our algorithm: it *always* produces BEC of the highest possible order n [for which $C_2(\delta_E = 0) = n!$]. This order is dictated by the number of particles in the most populated EEC, which in turn depends strongly on the location of a given EEC in phase-space, see Table II. It will significantly influence both the strength [as given by $C_2(\delta = 0)$] and the shape of the BEC effect, cf., Fig. 10. In it we show what happens when the maximal number of particles in each EEC is artificially limited so as not to exceed some im-

FIG. 10.   Comparison of $C_2(\delta E)$ for different maximally allowed sizes of EECs given by maximal number of particles n_{max} they can have. Notice the difference from the similar results obtained for pionic lattice and presented in Fig. 2(c). It is caused by the fact that here the distance between particles is not limited by the fixed spacing of the lattice as before.

posed maximal value equal to n_{max}. Notice that this requirement also affects the resulting number of EECs (the smaller population of EECs the more of them must be present). It is clear that this effect will be strongest in events with very high multiplicities recorded (cf. [41] for references to projects of the respective experiments). The sensitivity of our algorithm to n_{max}'s presented in Fig. 10 [for $C_2(\delta_{p_x})$ the changes are qualitatively the same for all choices of momenta presented here] makes it an ideal tool for numerical investigations of BEC also for particles satisfying statistics different than BE (for example, the so-called *parastatistics* [42]).
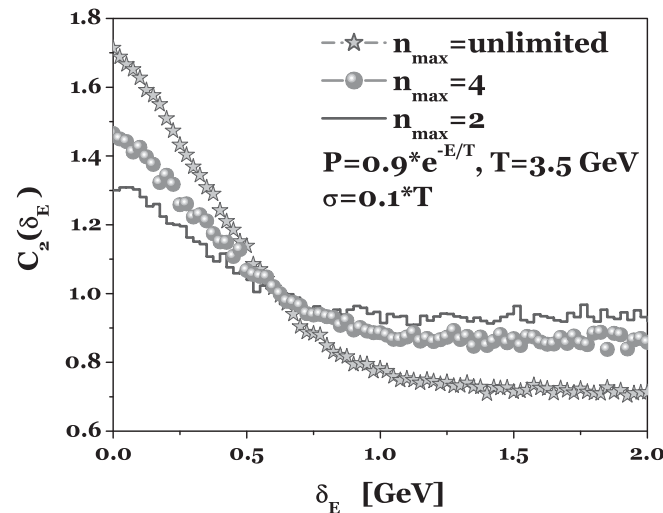
We close this section showing how sensitive $C_2(\delta_i)$ are to different choices of EECs represented by different values of parameters $\mathcal{P}_0$ and T and to different masses W of hadronizing source, cf. Fig. 11 and Table I (this is done again for $\sigma_0 = 0$ and using isotropic distributions of directions of momenta. Any changes in them, as discussed before, would then change these results accordingly in the way demonstrated in Figs. 6–8). The most characteristic feature is the observed growth of $C_2(\delta_i = 0)$ [i.e., the grow of the so-called "parameter of chaoticity" $\lambda = C_2(\delta_i = 0) - 1$] with a diminishing number of EECs, $\langle N_{cell} \rangle$. Actually, this result was behind the original introduction of the notion of EECs in describing the BEC effect done in [11] where the number of EECs is tightly connected with the parameter k in the NB multiparticle distributions used to fit data. An interesting feature of this approach, shared by our picture as well, is that, as shown in [11], it explains in a natural way the dependence of λ on dN/dy and on the atomic number of projectiles A [43]. In Appendix C we discuss changes in $C_2(\delta_i)$ introduced when correcting for the inevitable energy-momentum and charge imbalances induced by our algorithm.
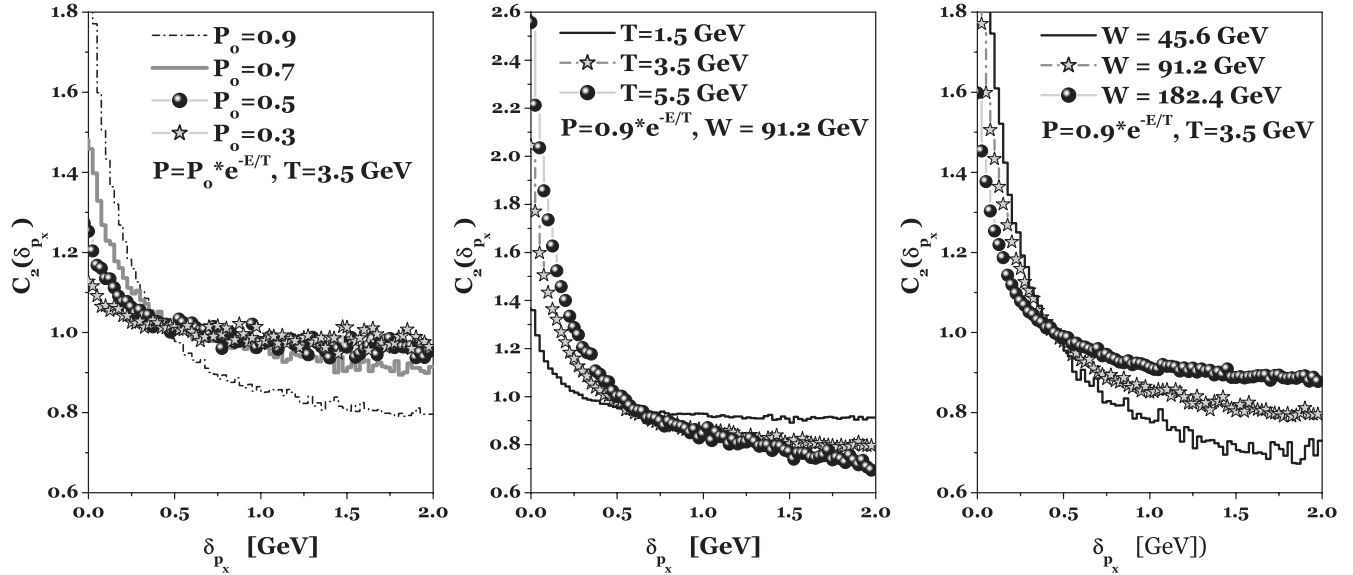
FIG. 11. Left panel and middle panel: sensitivity of $C_2(\delta_{p_x})$ to different choices of EECs exemplifying by different sets of parameters used. Right panel: the same but for different energies W and fixed size of EEC (as indicated, in all cases $\sigma_0 = 0$ and isotropic source was considered). The corresponding values of mean multiplicities, their dispersion as well as the mean number of EECs and their mean occupancies are listed in Table I.

C. Discussion

Let us recapitulate the physical picture we are proposing. Its basic object is an EEC, a quantum state containing a number of identical secondaries of the same, or nearly the same, energies. These secondaries are assumed to satisfy the BE statistics which is imposed by demanding that they follow geometric distribution. As a result, the correlation functions $C_2(\delta_X)$ that follow are very sensitive to the characteristics of the EEC, for example, the width of $C_2(\delta_X)$ is proportional to the allowed energy spread in an EEC, σ. It is best seen on the example of $C_2(\delta_E)$, cf. Fig. 6. Interestingly enough, when all particles in the EEC have the same energy $C_2(\delta_E)$ is divergent. On the other hand, in the same situation, correlation functions in momenta have already nonzero widths. This is because the choice $\sigma = 0$ does not constrain directions of momenta. The simplest case of isotropically selected directions, represented by $C_2(\delta_{p_x})$, is shown in Fig. 6. The choice of directions provides therefore additional freedom in modeling $C_2(\delta_{p_{x,z}})$. It can be seen in Figs. 7 and 8 where examples of restricting the range of transverse momenta and the choice of longitudinal momenta are displayed. As for the physical meaning of $\sigma > 0$, it is tempting to identify it with the temporal characteristic of the hadronization process, in fact with the life time of an average EEC.

So far we presented results only for direct pions being produced. To include resonances, one would first have to decide whether the BEC should affect them in the same way as particles or whether they affect only the pions resonances decay into. This point surely deserves further discussion, but it would bring us outside the scope of our paper. Therefore we present in Fig. 12 results for C_2

calculated for ρ mesons [of charges $(+, -, 0)$ and mass $m_\rho = 0.7$ GeV, with zero widths assumed for simplicity] considered to be simple particles subjected to the same
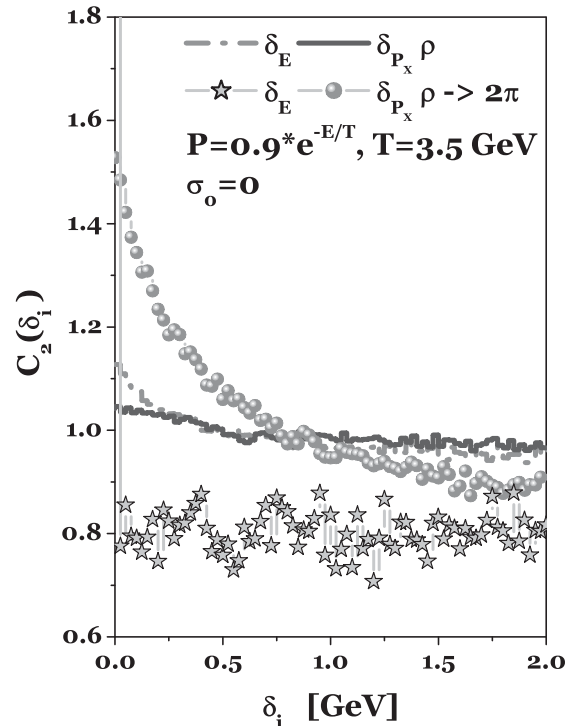

FIG. 12. Comparison of BEC for mesons ρ (with $m_\rho = 0.7$ GeV) and for pions obtained from their decays. To maximize the effect, we use the EEC for ρ's with fixed energies (i.e., $\sigma_0 = 0$). Both $C_2(\delta_E)$ and $C_2(\delta_{p_x})$ are presented. Notice that also for ρ correlation function $C_2(\delta_E)$ is concentrated in the first bin only.

procedure of building EECs as that for pions. This is compared with the case where such ρ's subsequently decay into pions. Notice that, whereas the BEC for ρ's is quite strong and not very much different from that for pions only, it hardly survives the process of ρ's decay, especially for the $C_2(\delta_{p_x})$ case. However, it must be stressed at this point that, so far, our ρ's were treated as spinless particles and that they were assumed to decay into pairs of pions in an isotropic way in their center of mass [44].

In our algorithm only particles in EECs are subjected to BEC, there are no intercorrelations of the BE type between particles from different EECs (see Appendix A). Such picture seems to be supported by recent data on BEC in $e^+e^- \rightarrow W^+W^-$ multi-W boson production which show nonexistence of inter-W BEC. This result suggests strongly that, although spatially located practically on top of each other, nevertheless bosons W act as *independent* sources of pions in this case [45].

We would like to stress here that all restrictions on energies and momenta mentioned above influence first of all the shape of a single EEC in momentum space rather than global characteristic of a given hadronizing source used. It is therefore to a large extent the EEC information on which are encoded in the correlation function C_2. On the other hand, their number depends in the first instance on the characteristics of the hadronizing source encoded in the choice of $f(E)$. Occupancy of EECs, however, depends strongly on $\mathcal{P}_0$ and together with T from $f(E)$ change substantially both the multiplicity distributions (in our case from the Poisson-like to Pólya-Aeppli

one) and single particle distributions as well (see Figs. 4 and 5).

It is worth mentioning at this point that together with BEC our algorithm introduces also some intermittency signal, much in the way expected already in [26], see Fig. 13. It depends noticeably on the smearing of EECs in energy and is very sensitive to the energy-momentum imbalance corrections (cf., Appendix C) [46].

IV. SUMMARY AND CONCLUSIONS

To summarize: we argue that proper numerical symmetrization of the multiparticle state of identical particles can be achieved in an economical way (in what concerns computational time) only by bunching them in phase-space in such a way that (identical) particles in each bunch (called here EEC—*elementary emitting cell*) have (almost) the same energies and follow a geometrical (Bose-Einstein) distribution. Only particles in EECs experience BEC, those from different cells do not (see Appendix A). We regard this conjecture as emerging in a natural way from previous investigations [4,12,14,15,47]. It is the main result of studies of a properly symmetrized multiparticle wave function of identical secondaries produced in the reaction [4,12,14]. They unravelled that in such a state the originally uniformly distributed particles start to bunch [4,14], also changing the original Poissonian multiplicity distribution to a NB one [4]. The similarity with the clan model [23] leading to QCM proposed here was then immediate. The same conjecture was achieved independently
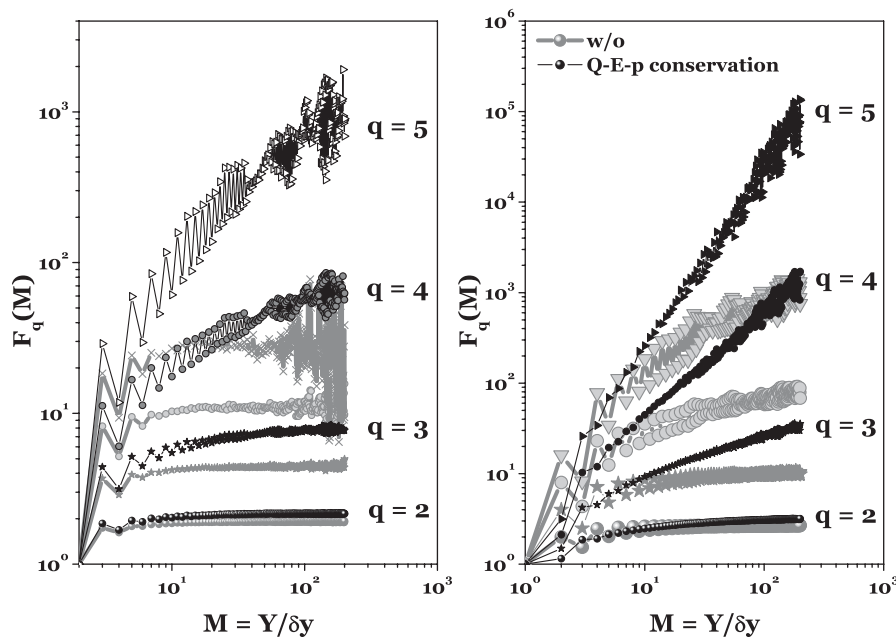

FIG. 13.   Example of intermittency signals obtained using our algorithm with $\mathcal{P}_0 = 0.9$, $T = 3.5$. Left panel: not corrected for energy-momentum and charge imbalances results for $\sigma_0 = 0$ (black curves) and $\sigma_0 = 0.3$ (gray curves) are compared. Right panel: results for $\sigma_0 = 0$ only with and without corrections (most of the visible effect comes from correcting the energy-momentum imbalance). Moments $F_q(M)$ are defined as in [58].

following studies in which one works with a number of quanta (particles) without invoking wave functions [28–30,32–35]. In the first practical application of the concept of bunching [15], the whole (one-dimensional) phase-space was divided into such EECs (of equal size in rapidity space) and this simple decision resulted in profound consequences for what concerns the ability to describe different physical distributions. We develop this idea further: our EECs are formed dynamically, they can both overlap each other and be widely separated from each other and their number and multiplicities (i.e., their sizes) of particles in them fluctuate from event to event. This work is then about how to form such EECs and what to do with them.

One can ask whether cells (or proper bunching of identical particles in phase-space, advocated here) are really needed to model quantum Bose statistics or, perhaps, it would be enough just to use the usual Bose-Einstein distributions to this aim. To answer this question, let us compare two ways of producing bosonic particles: (i) generating them directly from Bose-Einstein distribution [like $\langle N(E_i) \rangle$ as given in Eq. (14), which is the most simple way advocated on many occasions] and, (ii) generating particles from a Boltzmann distribution and bunching them in an appropriate way in phase-space according to QCM presented here. In the first case, one gets the correct single particle distribution, whereas in the second case one also accounts for multiparticle correlations of quantum statistical origin. The corresponding results are presented in Fig. 14. They show that both
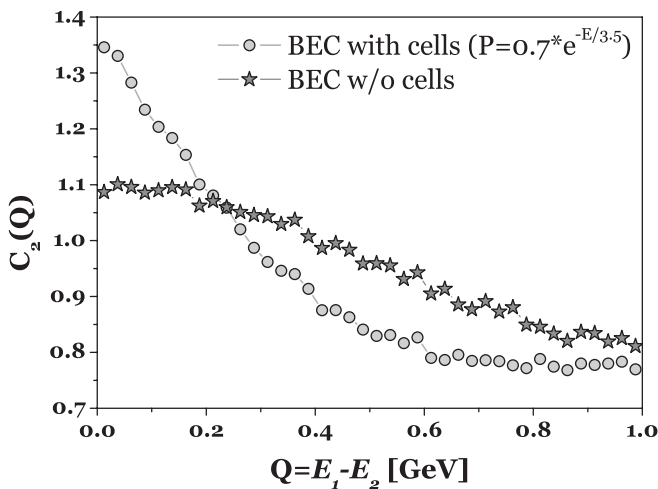

FIG. 14. Comparison of C_2 modeled by using MC event generators with EECs (circles) and without EECs but with selecting particles directly from the corresponding Bose-Einstein distribution $\langle N(E_i) \rangle$ as given in Eq. (14) [59]. In both cases the Boltzmann distribution for classical particles was used as a reference event. This fact may be crucial to get an apparent increase in the case of using directly Bose-Einstein distributions (as in [59]). The use of a mixed event instead, which will not affect substantially the result obtained using EECs, will most probably kill the other effect.

approaches lead to very different results, which can be understood by realizing that case (i) corresponds to a particular realization of case (ii), namely, with only one cell containing the same average number of particles. In fact, case (i) shows only some trivial correlations which can be eliminated by a proper choice of the reference distribution. Therefore, we argue that, according to our understanding, the better approach (after correcting additionally for charge and energy-momentum conservations) is that

$$BEC = cells + geometrical\ distribution. \qquad (20)$$

From its construction it is evident that our algorithm is best suited to study events with large multiplicities (as planned in some experiments [41]). The statement (20) also summarizes the only possible way to incorporate our algorithm in MCEG codes: according to our finding it should be done by enforcing particles to be produced in bunches with characteristics of our EECs. In fact, closer inspections on all previous efforts to imitate BEC mentioned in Sec. II A show that they all implicitly were aiming in a similar direction [16–20]. The difference was that they were trying to do it *a posteriori* rather than *a priori* and that their weighting procedure was aimed more at the spatiotemporal (unknown) characteristics of the hadronizing source than on the true physical principles of BEC.

In this work we have stopped short of a general comparison with data. The reason is that we were using here a most simple statistical model of hadronization in order to illustrate our algorithm. According to it, a hadronizing source is assumed to be a single object with some fixed mass W and fixed initial charge, which is the situation encountered only in e^+e^- annihilation reactions. In all other multiparticle production processes, one either encounters W varying from event to event (following some distribution, for example, inelasticity distribution [48]) or there is a number of hadronizing sources with different W in each event (which is the most probable situation in heavy ion collisions). Moreover, the statistical scheme of hadronization employed here means that our hadronizing source does not experience any internal flows and is not subjected to any external force, which would result in some energy-position correlations or specific effects of partial coherence (cf., [9]) and thus additionally influence the C_2 correlation function. The problem of the possible net charges of such subsources was never discussed. All this asks for a very specialized study, which goes outside the scope of this paper. What we can only say at this moment is that, when undertaken, such a study would mean the necessity of developing our formalism further in what concerns details of modeling EECs mentioned before. The most probable approach would be to *additionally assume* that each EEC itself should be described by a *properly symmetrized* n_{part}-*particle wave function* (where n_{part} is the number of particles in this EEC). Only then would one be

able to introduce into the model a characteristic momentum-positions correlation caused by quantum statistics [much in the spirit leading to Eq. (1)]. The price for following such a procedure is the necessity to also introduce to our description the space-time characteristics of the hadronizing source, which we were not dealing with so far. This would result in the same permanent structure as given by Eq. (2), but with much smaller sizes and with explicit dependence on spatiotemporal variables [as in Eq. (8)] to be used later when selecting momenta (actually, they would be effectively integrated out in this procedure). However, the noticeable feature is that in our case this procedure would not demand the spatiotemporal factorization property of the hadronizing source assumed in (1). When replacing plane waves used there by Coulomb distorted wave functions [49] (which is common practice nowadays), one could then attempt, in principle, to account for the influence of Coulomb interactions so far neglected here (albeit only on the level of 2-body interactions). This is, of course, not the only possible generalization and therefore we leave the problem of confrontation with real data for further studies. Finally, let us notice that any serious comparison with data would have to be done including corrections for energy-momentum and total charge imbalances induced by our algorithm, which (as seen in Appendix C) can be quite substantial and not unique.

Let us close by noticing that, although our algorithm was originally intended to model quantum phenomena of BEC only, it is in fact more general. The reason is that the characteristic structure of the C_2 correlation function associated with specific bunching of identical particles turns out to be a quite universal phenomenon also observed in many other, purely classical systems, provided only that they exhibit strong and correlated fluctuations [50]. This means then that our algorithm, albeit with different motivation, could also be applied there. At this point, one should also notice an attempt at numerical modeling of another quantum phenomenon, namely, Bose-Einstein *condensation* presented in [51] and the possible connection of the above with the physics of networks [52]. Finally, we also claim that, because of its sensitivity to maximal occupancy of EECs, our method could easily be modified to be able to study BEC effects for parabosons [42].

ACKNOWLEDGMENTS

APPENDIX A: SOME REMARKS ON EECS

We would like to comment in more detail on our proposition that identical bosons should come in EECs and experience effects of BEC there, whereas no such effects should be seen when bosons from different cells are considered. In the language used in [53], the probability of registration of a coincidence of n bosons in states $j_1, \ldots, j_n$ is given by a normalized correlation tensor of rank $2n$,

$$g^{(nn)}_{j_1 \ldots j_n j_{n+1} \ldots j_{2n}} = \frac{G^{(nn)}_{j_1 \ldots j_n j_{n+1} \ldots j_{2n}}}{\prod_{i=1}^{2n} \sqrt{G^{(11)}_{j_i, j_i}}}, \tag{A1}$$

where $G^{(nm)}_{j_1 \ldots j_n j_{n+1} \ldots j_{n+m}} = \mathrm{Tr}\{\rho a^\dagger_{j_1} \ldots a^\dagger_{j_n} a_{j_{n+1}} \ldots a_{j_{n+m}}\}$

is given in terms of the density matrix operator ρ, whereas $a^\dagger$ and a are, respectively, creation and annihilation operators. If

$$|g^{(nn)}_{j_1 \ldots j_{2n}}| = 1 \qquad n \le N, \tag{A2}$$

we have coherence of the order $2N$. Experimentally this means that the probability of registering n bosons in coincidence is equal to the product of probabilities to register individual ones. Because of commutation relations for bosons, $[a_k, a_l] = [a^\dagger_k, a^\dagger_l] = 0$ and $[a_k, a^\dagger_l] = \delta_{kl}$, one has that $a^\dagger_k a^\dagger_l a_k a_l = a^\dagger_l a^\dagger_k a_k a_l = a^\dagger_k a^\dagger_l a_l a_k = a^\dagger_l a^\dagger_k a_l a_k = n_k n_l$ and then from Eq. (A1) that for two bosons from different states

$$g^{(22)}_{k_1 l_1 k_2 l_2} = \frac{\overline{n_k n_l}}{\overline{n_k} \cdot \overline{n_l}} = \frac{\overline{n_k} \cdot \overline{n_l}}{\overline{n_k} \cdot \overline{n_l}} = 1. \tag{A3}$$

This means that two bosons from different states (in our case: from different EECs) exhibit second order coherence. On the other hand, in the situation in which only one state k is occupied, i.e., when $a^\dagger_k a^\dagger_k a_k a_k = a^\dagger_k a_k a^\dagger_k a_k - a^\dagger_k a_k = n^2_k - n_k$, Eq. (A1) results in

$$g^{(22)}_{k_1 k_1 k_2 k_2} = \frac{\overline{n^2_k} - \overline{n_k}}{\overline{n_k} \cdot \overline{n_k}} = \frac{2\overline{n_k}^2}{\overline{n_k} \cdot \overline{n_k}} = 2 \tag{A4}$$

(here we use the fact that in geometrical distribution $\overline{n^2_k} - \overline{n_k}^2 = \overline{n_k}(1 + \overline{n_k})$). Notice that it is greater by unity than (A3) but, because g is not limited, it cannot serve as a degree of coherence. On the other hand, we can write following Sec. II C the true correlation function C_2 as

$$C_2 = \frac{\overline{n(n-1)}}{\bar{n}^2} = 1 + \frac{\mathrm{Var}(n)}{\bar{n}^2} - \frac{1}{\bar{n}}, \tag{A5}$$

where $\mathrm{Var}(n) = \mathrm{Var}(n_k) = \bar{n}(1 + \bar{n})$ for bosons from the same state, which in our case means from the same EEC. This immediately leads to $C_2 = 2$ in this case [for Boltzmann statistics $\mathrm{Var}(n) = \bar{n}$ and one gets $C_2 = 1$ instead]. For k EECs we have multiplicity distribution in NB form with variance $\mathrm{Var}(n) = k\mathrm{Var}(n_k) = \bar{n} + \bar{n}^2/k$ and mean multiplicity $\bar{n} = k\bar{n}_k$. This leads immediately to $C_2 = 1 + 1/k$, i.e., we have $C_2 = 2$ for $k = 1$ and $C_2 \to 1$ for $k \to \infty$.

TABLE III. Schematic presentation of how a different form of commutation relation in a quantum field theoretical description of BEC results in a different form of C_2 function [9]. The actual form of C_2 [i.e., of the function $\mathfrak{g}(Q \cdot R)$] depends on the form of function $\Delta(\cdots)$ used to moderate the original $\delta(\cdots)$ function.

Volume (4 dim)	Wave function	Commutation relation $[\hat{c}(p_\mu), \hat{c}(p'_\nu)]$	Correlation function $C_2(Q) - 1$
$V \to \infty$	$e^{-ip_\mu \cdot x^\mu}$	$\delta^4(p_\mu - p'_\nu)$	$\delta(Q \cdot R)$
$V = V_0$	$e^{-ip_\mu \cdot x^\mu - (1/2\sigma_p^2)p^2}$	$\propto \Delta^4(p_\mu - p'_\nu)$	$\mathfrak{g}(Q \cdot R)$

APPENDIX B: STRUCTURE OF $C_2(Q)$ AND FINITENESS OF HADRONIZING SOURCE

As demonstrated in [9], using a quantum field theory approach to BEC, the structure of the correlation function $C_2(Q)$ is connected with the finiteness of the hadronizing source. In the four-dimensional case, the wave function formalism with $\exp(-ip_\mu \cdot x^\mu)$ implies the infinite (4-dimensional) volume of the hadronizing source, $V \to \infty$. This can then be connected to the fact that commutation relations for the respective operators contain delta functions,

$$[\hat{c}(p_\mu), \hat{c}(p'_\nu)] = \delta^4(p_\mu - p'_\nu), \tag{B1}$$

which are nonzero only for identical values of the four-momenta (i.e., also energies), . They in turn lead to correlation functions $C_2(Q)$ in the form of

$$C_2(Q) = 1 + \delta(Q \cdot R), \tag{B2}$$

i.e., to $C_2(Q) > 1$ but only at one point, $Q = 0$ (cf., Table III).

However, as shown in [9], assuming commutation relations in the form of some sharply piked (but not infinite) functions Δ, i.e., replacing delta functions by functions with supports larger than limited to a one point only,

$$[\hat{c}(p_\mu), \hat{c}(p'_\nu)] \propto \Delta^4(p_\mu - p'_\nu), \tag{B3}$$

results immediately in the correlation function endowed with final width:

$$C_2(Q) = 1 + \mathfrak{g}(Q \cdot R) \tag{B4}$$

where the form of $\mathfrak{g}(Q \cdot R$ is a straightforward reflection of the assumed form of $\Delta^4(p_\mu - p'_\nu)$). Such a procedure corresponds to introducing a finite dimension of the source, $V = V_0$ [and the use of wave packets formalism, $\exp[-ip_\mu \cdot x^\mu - p^2/(2\sigma_p^2)]$, instead of plane waves].

APPENDIX C: CORRECTING FOR ENERGY-MOMENTUM AND CHARGE IMBALANCES

Any random selection procedure, even when following formulas which assume exact energy-momentum and charge conservations, frequently induces some energy-momentum and charge imbalances and this is also true in the case of our algorithm [54]. The obvious remedy would be to only accept events preserving the initial values of energy-momentum and charge. This, however, would result in an unacceptable long computational time. To the best of our knowledge, only in the algorithm presented in Sec. II B 3 [15] is energy-momentum assured using this method (with <20% accuracy) and charges are conserved
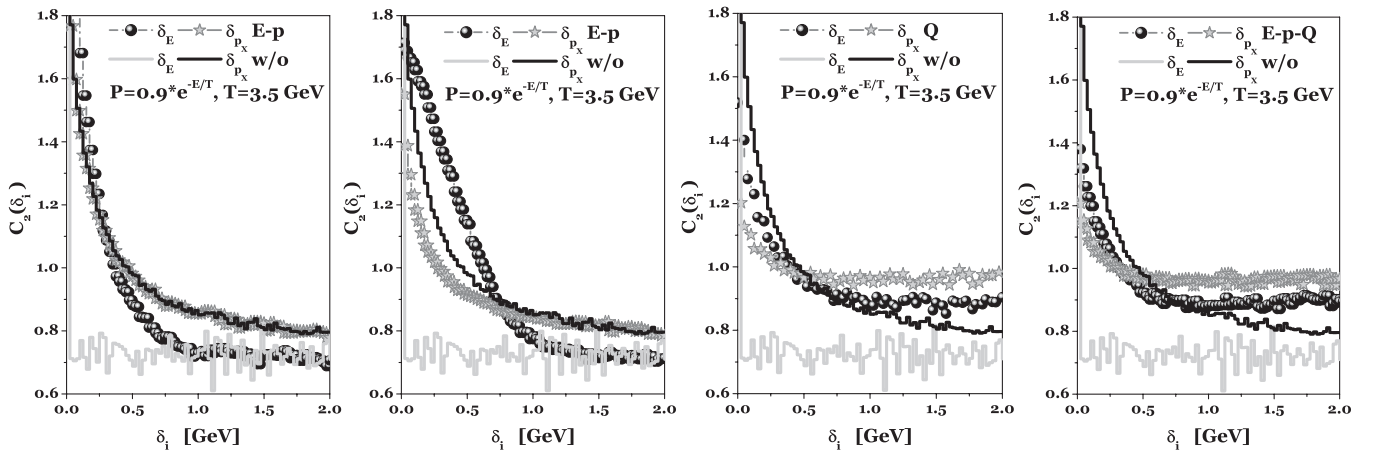

FIG. 15. Effects of correcting for the imbalances introduced by our selection procedure in energy-momentum (the first two panels from the left and the right panel) and total charge (the last two panels). Results without (w/o) corrections are the same at all panels. Two selections of the $(+ / -)$ sign of the p_L component are used: it is chosen randomly for each particle irrespective to the EEC it belongs to (all panels except the first from the left); all particles in a given EEC possess p_L of the same sign (left panel). In all panels the first bin of the gray full curve contains uncorrected $C_2(\delta_E)$. In all cases $\sigma_0 = 0$.

by accepting only events reproducing the initially assumed charge. Results of all other algorithms presented here were prepared in the same way as what we have presented, i.e., not corrected for any, therefore they can be compared with each other. We would now like to discuss changes in correlation functions induced by correcting for energy-momentum and charge imbalances introduced in the selection process. At first, one must stress that there is no unique procedure to perform such corrections [55]. In what follows we shall use a very simple (but fast) procedure: (i) shifting (by the same amounts, Δp_x, Δp_y and Δp_z) components of momenta, $p_{x,y,z}$ and, after balancing momenta, appropriately rescaling energies; (ii) by converting the necessary number of (+) particles to (−) ones (or vice versa, depending on the actual charge balance in the event) and, in case of odd number of particles with surplus charge, attribute the surplus charge to some randomly chosen (0) charged particle.

The results are shown in Fig. 15 (our hadronizing sources have zero initial charge). The most sensitive to the correcting procedure is $C_2(\delta_E)$, correlations of momenta feel corrections only when all particles in a given EEC are located in the same hemisphere. Otherwise there is essentially no difference, The reason for such behavior is that, in the other case, the relative differences of momenta considered here are not changed by the shifting procedure. In correcting for $\Delta Q \neq 0$, the EECs with single particle only were chosen first, afterwards EECs with $N_{\text{part}} > 1$ were chosen randomly until the correct balance of charge was achieved. In this case, as one can see in Fig. 15 (lower panels), the effect is quite dramatic and essentially independent of the way the momenta were chosen or on their energy-momentum balance. The best measure of this is provided by the widening of the originally δ-like $C_2(\delta_E)$. Notice also the clearly visible upward bending of the tail of C_2 distributions. It is worth noticing at this point that similar shapes are observed in C_2 obtained from e^+e^- annihilation experiments, in which, as in the case considered here, the original energy and total charges are well known and fixed.

Effects shown here are so dramatic because, in order to be as near as possible to the proper BE distributions in the average EEC in the situation of only limited energy W available for hadronization, we had maximized sizes of EECs by allocating to them many particles; this was technically achieved by using a large value of parameter $\mathcal{P}_0$, $\mathcal{P}_0 = 0.9$. It resulted in a very broad total charge distribution (centered on the assumed value $Q_{\text{TOT}} = 0$), see
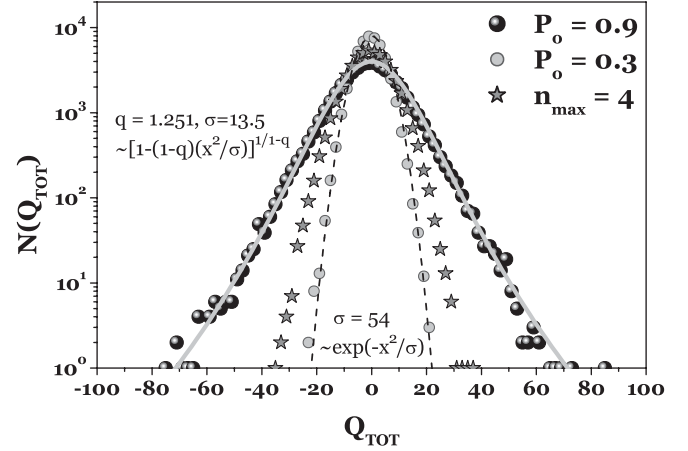

FIG. 16.   Typical distributions of total charges obtained from our selection procedure performed for $W = 91.2$ GeV, $T = 3.5$ GeV, and $\sigma_0 = 0.$ for different sizes of EECs as dictated by parameter $\mathcal{P}_0 = 0.9$ and $\mathcal{P}_0 = 0.3$ and for maximal size of EECs artificially limited to $n_{\text{max}} = 4$ (for $\mathcal{P}_0 = 0.9$). The best fits to most narrow and most wide distributions are shown. Total initial charge of hadronizing mass W was assumed $Q = 0$.

Fig. 16. The reason for such large fluctuations is as follows. In our algorithm each EEC contains particles of the same charge $(+, -, 0)$ selected randomly (with equal probabilities). With only one particle per EEC, $N_{\text{part}} = 1$, this would result in quite narrow ΔQ_{EEC}. However, because in general $N_{\text{part}} > 1$ and fluctuates, the charge imbalance ΔQ_{EEC} broadens considerably to what is observed in Fig. 16. It leads then to very large fluctuations and events with large charge imbalance are quite frequent. The effect is therefore, as seen in Fig. 16, very sensitive to the size of EECs allowed (see Fig. 4 and Table I), i.e., to the parameter $\mathcal{P}_0$ responsible for N_{part} and to any attempts to limit it as, for example, shown in Fig. 10 [56].

To summarize: this problem arises because our procedure destroys part of the originally formed EECs and forms some new ones which results in the sensitivity observed. On the other hand, we do not see at the moment any economical way to account for extremely complicated correlations arising when attempting to keep $Q_{\text{TOT}} = 0$ all the time. The only apparent cure, to keep only events with exactly right charge balance, would place our algorithm in the same category (in what concerns the use of computational time) as those presented in Secs. II B 1 and II B 2 [4,14] (which, by the way, were not attempting to impose any conservation laws at all).

---

[1] Compare QM05 Proceedings, Nucl. Phys. A774 (2006); for specialized reviews, see also K. J. Eskola, Nucl. Phys. **A698**, 78 (2002); or S. A. Bass *et al.*, Prog. Part. Nucl. Phys. **41**, 255 (1998).

[2] G. Goldhaber *et al.*, Phys. Rev. Lett. **3**, 181 (1959); Phys. Rev. **120**, 300 (1960).

[3] In fact, at the beginning the observed effect was called *GGLP effect* in distinction to an apparently similar effect observed in astronomy and known as *HBT effect* which was used to obtain stellar dimensions, see T. J. Humanic, Int. J. Mod. Phys. E **15**, 197 (2006) for most recent review and references therein. Other important reviews are in [6] whereas pedagogical descriptions of BEC are provided in [7,8]. Finally, in [27] one can find a valuable collection of seminal papers concerning different aspects of BEC.

[4] W. A. Zajc, Phys. Rev. D **35**, 3396 (1987).

[5] It means that the unobserved yield acts as a kind of heath bath influencing measured observables. Actually this is the main origin of the known spectacular success of the statistical description of such reactions with temperature T being the most important parameter describing the influence of such a heath bath, see G. Wilk, hep-ph/0610292 [Braz. J. Phys. (to be published)], and references therein.

[6] U. A. Wiedemann and U. Heinz, Phys. Rep. **319**, 145 (1999); R. M. Weiner, Phys. Rep. **327**, 249 (2000); T. Csörgő, Acta Phys. Hung. A–Heavy Ion Phys. **15**, 1 (2002); *Particle Production Spanning MeV and TeV Energies*, edited by W. Kittel *et al.*, NATO Science Series C Vol. 554 (Kluwer Academic, Dordrecht, 2000), p. 203; W. Kittel, Acta Phys. Pol. B **32**, 3927 (2001); G. Alexander, Rep. Prog. Phys. **66**, 481 (2003).

[7] W. A. Zajc, in *Particle Production in Highly Excited Matter*, edited by H. H. Gutbrod and J. Rafelski (Plenum Press, New York, 1993), p. 435.

[8] R. M. Weiner, *Introduction to BEC and Subatomic Interferometry* (Wiley, New York, 1999).

[9] G. A. Kozlov, O. V. Utyuzh, and G. Wilk, Phys. Rev. C **68**, 024901 (2003); Ukr. J. Phys. **48**, 1313 (2003).

[10] Closer inspection [7] reveals that one rather gets in this way a Fourier transform of distributions of spatiotemporal two-particle separations (or *correlation lengths* [6]). Recently the possibility of sort of *imaging* the hadronization region by using data on C_2 has been pursued, see D. A. Brown *et al.*, Phys. Rev. C **72**, 054902 (2005), and references therein.

[11] M. Biyajima, N. Suzuki, G. Wilk, and Z. Włodarczyk, Phys. Lett. B **386**, 297 (1996).

[12] H. Merlitz and D. Pelte, Z. Phys. A **357**, 175 (1997). Compare also U. A. Wiedemann *et al.*, Phys. Rev. C **56**, R614 (1997); T. Csörgő and J. Zimányi, Phys. Rev. Lett. **80**, 916 (1998); Acta Phys. Hung. A–Heavy Ion Phys. **9**, 241 (1999).

[13] H. Merlitz and D. Pelte, Z. Phys. A **351**, 187 (1995).

[14] J. G. Cramer, ''Event Simulation of High-Order Bose-Einstein and Coulomb Correlations'' (University of Washington, 1996, unpublished).

[15] T. Osada, M. Maruyama, and F. Takagi, Phys. Rev. D **59**, 014024 (1998).

[16] K. Fiałkowski, R. Wit, and J. Wosiek, Phys. Rev. D **58**, 094013 (1998); T. Wibig, Phys. Rev. D **53**, 3586 (1996); B. Andersson, Acta Phys. Pol. B **29**, 1885 (1998); K. Geiger, J. Ellis, U. Heinz, and U. A. Wiedemann, Phys. Rev. D **61**, 054002 (2000); Q. H. Zhang, U. A. Wiedemann, C. Slotta, and U. Heinz, Phys. Lett. B **407**, 33 (1997).

[17] B. Andersson and M. Ringner, Nucl. Phys. **B513**, 627 (1998).

[18] L. Lönnblad and T. Sjöstrand, Eur. Phys. J. C **2**, 165 (1998).

[19] O. V. Utyuzh, G. Wilk, and Z. Włodarczyk, Phys. Lett. B **522**, 273 (2001).

[20] O. V. Utyuzh, G. Wilk, and Z. Włodarczyk, Acta Phys. Pol. B **33**, 2681 (2002).

[21] O. V. Utyuzh, G. Wilk, and Z. Włodarczyk, in *Proceedings of the XXXII ISMD, Alushta, Crimea, Ukraine, 2002*, edited by A. Sissakian, G. Kozlov, and E. Kolganova, [Acta Phys. Polon. B 33, 2681 (2002)].

[22] The only discussion of such changes we are aware of is in [19,20] where it was shown that an enforcing effect of BEC into a simple cascade model results in the appearances of multicharged vertices, not present in the original scheme. For more details, see [47] and references therein.

[23] A. Giovannini and L. Van Hove, Z. Phys. C **30**, 391 (1986); see also P. Carruthers and C. S. Shih, Int. J. Mod. Phys. A **2**, 1447 (1987).

[24] U. A. Wiedemann, P. Foka, H. Kalechofsky, M. Martin, C. Slotta, and Q. H. Zhang, Phys. Rev. C **56**, R614 (1997); M. Martin, H. Kalechofsky, P. Foka, and U. A. Wiedemann, Eur. Phys. J. C **2**, 359 (1998).

[25] The reason is obvious. When only mean multiplicity $\bar{n}$ is fixed, the most probable distribution according to the IT approach is a geometrical (or Bose-Einstein) one. Such is therefore distribution of particles in each cell in rapidity, therefore their composition will result in $P(n)$ of NB type [23].

[26] Actually one obtains in this way only some part of this intermittency signal. Nevertheless this fact suggests that fluctuations connected with intermittency [58] are, at least to some extent, the same as those caused by BEC (or both have the same origin), cf. P. Carruthers, E. M. Friedlander, C. C. Shih, and R. M. Weiner, Phys. Lett. B **222**, 487 (1989) and [8].

[27] R. M. Weiner, *Bose-Einstein Correlations in Particle and Nuclear Physics* (Wiley, New York, 1997), collection of selected articles.

[28] K. Zalewski, Nucl. Phys. B, Proc. Suppl. **74**, 65 (1999); Lect. Notes Phys. **539**, 291 (2000).

[29] E. E. Purcell, Nature (London) **178**, 1449 (1956). Compare also L. Mandel, E. C. G. Sudarshan, and E. Wolf, Proc. Phys. Soc. **84**, 435 (1964).

[30] A. Giovannini and H. B. Nielsen, The Niels Bohr Institute Report No. NBI-HE-73-17 (unpublished). See also Proceedings of the IV International Symposium on Multiparticle Hadrodynamics, Pavia, 1973, edited by F. Duimio, A. Giovannini, and S. Ratii, p. 538.

[31] Notice that, in general, the multiplicity distribution function satisfies the relation: $P(n + 1)/P(n) = g(n)/(n + 1)$, where $(n + 1)$ is a reflection of the fact that with n particles given the $(n + 1)$th one can be allocated in $n + 1$ ways. Different $g(n)$ result in different forms of $P(n)$. In particular, for $g(n) = a$ one gets (after normalization) $P(n) = a^n e^{-a}/n!$, whereas $g(n) = p(n + 1)$ results (after normalization) in $P(n) = (1 - p)p^n$, i.e., in a geometrical distribution, which means that the emission of an extra particle is enhanced by a factor $(n + 1)$ and this is Bose-

Einstein enhancement and the emission with this is usually called stimulated emission [30].

[32] See, for example, R. Loudon, *The Quantum Theory of Light* (Clarendon Press, Oxford, 1983), 2nd ed.; J. W. Goodman, *Statistical Optics* (Wiley, New York, 1985).

[33] M. Biyajima, Prog. Theor. Phys. **69**, 966 (1983); Phys. Lett. **137B**, 225 (1984).

[34] W. J. Knox, Phys. Rev. D **10**, 65 (1974); E. H. De Groot and H. Satz, Nucl. Phys. **B130**, 257 (1977); J. Kripfganz, Acta Phys. Pol. B **8**, 945 (1977); A. M. Cooper, O. Miyamura, A. Suzuki, and K. Takahashi, Phys. Lett. **87B**, 393 (1979); F. Takagi, Prog. Theor. Phys. Suppl. **120**, 201 (1995).

[35] K. Fiałkowski, in *Proceedings of the XXX ISMD, Tihany, Hungary, 2000*, edited by T. Csörgő *et al.* (World Scientific, Singapore, 2001), p. 357; M. Stephanov, Phys. Rev. D **65**, 096008 (2002).

[36] In fact all this is true only for an *a priori* unlimited number of trials. In reality, because the pool of available particles is $N \leq N_{tot}$ (where N_{tot} is limited by the available energy W), one gets $P_{N_{tot}}(N) = (1 - P)P^N/[1 - P^{(N_{tot}+1)}]$ and $\langle N \rangle_{N_{tot}} = \langle N \rangle_\infty [1 - P^{N_{tot}}]/[1 - P^{(N_{tot}+1)}] - N_{tot}P^{(N_{tot}+1)}/[1 - P^{(N_{tot}+1)}]$, where $\langle N \rangle_\infty$ is given by Eq. (11). It means that Eq. (14) will also be modified accordingly.

[37] R. Kacker and I. Olkin, J. Res. Natl. Inst. Stand. Technol. **110**, 67 (2005).

[38] J. Finkelstein, Phys. Rev. D **37**, 2446 (1988); Ding-wei Huang, Phys. Rev. D **58**, 017501 (1998).

[39] It is interesting to notice at this point that the best fits to $C_2(\delta_E)$ and $C_2(\delta_{p_x})$ for $\sigma_0 = 0.1$ presented here can be obtained by using, respectively [$x = \delta_i$ and $y = C_2(\delta_i)$], shifted Gaussian $y = y_0 + \sqrt{2/\pi} A \exp[-2(x - x_c)^2/w^2]/w$ (with $y_0 = 0.724$, $x_c = -0.125$, $w = 0.922$, and $A = 1.186$), and shifted Lorentzian $y = y_0 + (2Aw/\pi)/[4(x - x_c)^2 + w^2]$ (with $y_0 = 0.744$, $x_c = 0.0003$, $w = 1.221$, and $A = 1.154$). Notice that the later shape belongs to the category of Lévy distributions discussed in the context of BEC in T. Csörgő, S. Hegyi, and W. Zajc, Eur. Phys. J. C **36**, 36 (2004) because of their connection with the possible fractality of the hadronizing source. In fact one could as well use other forms of the $G(E)$ function in Eq. (18) to get still another form of C_2, see, for example, T. Mizoguchi, M. Biyajima, and T. Kageya, Prog. Theor. Phys. **91**, 905 (1994); [for more details cf. AIP Conf. Proc. **828** (2006)].

[40] I. V. Andreev, M. Plümer, B. R. Schlei, and R. M. Weiner, Phys. Rev. D **49**, 1217 (1994).

[41] V. V. Begun and M. I. Gorenstein, hep-ph/0611043; for references to high multiplicity measurement projects, see E. Kokoulina, A. Kutov, and V. Nikitin, hep-ph/0612364 [Braz. J. Phys. (to be published)].

[42] See, for example, A. M. Gavrilik, Symm., Integ. Geom., Meth. Appl. **2**, 074 (2006); Ch. A. Nelson and P. R. Shimpi, math-ph/0610075.

[43] This should be contrasted, for example, with the concept of resonant "halo" discussed in S. Nickerson, T. Csörgő, and D. Kiang, Phys. Rev. C **57**, 3251 (1998), which is not able to do so.

[44] Notice that the problem of how to account for the possibly nonzero spin of produced resonances is highly nontrivial. In principle, one should build EECs with particles pos-

sessing either the same helicity (but then they would all have to possess momenta pointing in the same direction) or with the same projection of spins (but then one would have to choose the external axis and choose not energies, as we are doing so far, but rather momenta). In both cases it would result in a completely different approach, which we shall not pursued here.

[45] See, for example, O. Pooth (OPAL Collaboration), Nucl. Phys. B, Proc. Suppl. **152**, 35 (2006), and references therein.

[46] This is a potentially very interesting result deserving further specialized consideration, which, however, would lead us outside the scope of the present paper. In this respect, we refer to the work by E. K. G. Sarkisyan, Phys. Lett. B **477**, 1 (2000), where different multiplicity distributions were studied from the point of view of intermittency and higher-order correlations. Similarly, in G. Abbiendi *et al.* (OPAL Collaboration), Phys. Lett. B **523**, 35 (2001), one can find studies of intermittency and especially of the higher-order genuine correlations made with an all-charge vs like-sign group of hadrons compared to the Bose-Einstein effect.

[47] O. V. Utyuzh, G. Wilk, and Z. Włodarczyk, AIP Conf. Proc. **828**, 75 (2006); Nukleonika (Supplement 2) **49**, S33 (2004); Acta Phys. Hung. A-Heavy Ion Phys. **25**, 83 (2006); Nukleonika (Supplement 3) **51**, S105 (2006).

[48] T. Osada, O. V. Utyuzh, G. Wilk, and Z. Włodarczyk, Eur. Phys. J. B **50**, 7 (2006), and references therein.

[49] M. Biyajima, T. Mizoguchi, T. Osada, and G. Wilk, Phys. Lett. B **353**, 340 (1995); **366**, 394 (1996); see also the review by O. V. Utyuzh, AIP Conf. Proc. **828**, 595 (2006).

[50] Compare, for example, A. E. Ezhov and A. Yu. Khrennikov, Phys. Rev. E **71**, 016138 (2005); K. Stalinas, cond-mat/0001436; cond-mat/0001347.

[51] R. Kutner and M. Regulski, Comput. Phys. Commun. **121–122**, 586 (1999); cf. also R. Kutner, K. W. Kehr, W. Renz, and R. Przeniosło, J. Phys. A **28**, 923 (1995).

[52] G. Bianconi and A.-L. Barabási, Phys. Rev. Lett. **86**, 5632 (2001).

[53] R. J. Glauber, Rev. Mod. Phys. **78**, 1267 (2006), and references therein.

[54] That this point can be important is demonstrated, for example, in N. Borghini, Eur. Phys. J. C **30**, 381 (2003) and Phys. Rev. C **75**, 021904 (2007); B. B. Back, Phys. Rev. C **72**, 064906 (2005) or in Z. Chajęcki and M. Lisa, nucl-th/0612080.

[55] For example, the sequential choice of energies from the distribution $f'(E) = E \cdot f(E)$ would result in an event reproducing the initial distribution $f(E)$ and conserving energy [because sampling from uniform distribution $x_k \in [0, 1 - x_1 - x_2 - \cdots - x_{k-1}]$ results in $P(x) = 1/x$, cf., M. Shibata, Phys. Rev. D **24**, 1847 (1981)]. This could be thought as a natural method to follow. However, it turns out that one cannot correct imbalances in momenta $p_{x,y,z}$ just by rotating all angles by some fixed $(\Delta\Theta, \Delta\Phi)$, the rescaling of at least one component is necessary. This ruins the original energy balance and needs further corrections.

[56] It is interesting to note that distributions of Q_{TOT} in Fig. 16 follow Gaussian form for small $\mathcal{P}_0$, for $\mathcal{P}_0 = 0.9$ which becomes the so-called q-Gaussian distribution (known

from Tsallis statistics, see reference in [5]).

[57] P. Abreu *et al.* (DELPHI Collaboration), Phys. Lett. B **286**, 201 (1992); **247**, 137 (1990).

[58] E. A. De Wolf, I. M. Dremin, and W. Kittel, Phys. Rep. **270**, 1 (1996); P. Bożek, M. Płoszajczak, and R. Botet, *ibid.* **252**, 101 (1995); I. V. Andreev, I. M. Dremin, M. Biyajima, and N. Suzuki, Int. J. Mod. Phys. A **10**, 3951 (1995).

[59] A. Kisiel, T. Tałuć, W. Broniowski, and W. Florkowski, Comput. Phys. Commun. **174**, 669 (2006).